Universität für Bodenkultur Wien

University of Natural Resources and Life Sciences, Vienna

Department of Water, Atmosphere and Environment

Institute of Hydraulics and Rural Water Management

Simulation of Surface Runoff and Soil Erosion of a Watershed in Northern Ethiopia

Application and Verification of the SWAT Model for two small Agricultural Watersheds in the Gumara-Maksegnit Watershed

Thesis submitted in partial fulfillment of the requirements for the degree of Diplomingenieur in Watermanagement and Environmental Engineering

by

Roman SCHIFFER

Supervisor: Ao.Univ.Prof. Dipl.-Ing. Dr.nat.techn. Andreas Klik

Co-Supervisor: Dr. Raghavan Srinivasan, Ph.D., P.E.

Co-Supervisor: Ao.Univ.Prof. Dipl.-Ing. Dr.nat.techn. Hubert Holzmann

BOKU registration number: 0840229

June 2015

Acknowledgements

This master thesis would not have been possible without the support of many people throughout the research for and writing of this thesis.

First, I want to thank my supervisor Andreas Klik for providing me with the opportunity to be part of this project and the possibility to do research abroad and gain insights in a very fascinating research field. Further I want to express my gratitude to Raghavan Srinivasan from Texas A&M University. He introduced me to the use of SWAT and guided me through my research, especially during my stay at Texas A&M University. I also want to thank Stefan Strohmeier from ICARDA whose insights and support were of exceedingly great value for this study.

Special thanks go to Hailu Kendie and Nigus Demelash from GARC who provided me with data and essential information regarding the study area.

I want to sincerely thank my parents who provided me with the opportunity to pursue my studies and gave me the freedom I needed throughout this process. I also want to thank my two sisters and my friends for their continuous support and encouragement. Finally I want to thank Alenka for believing in what I was doing and her constant emotional support from the very beginning.

Abstract

Land degradation is a major issue in the Ethiopian Highlands. Deforestation leads to ongoing soil erosion during the rainy season and thus the hydrology of a watershed changes as high erosion rates and dense gully networks cause a direct drainage of rain water usable for crop production. The application of hydrological models can provide a link between local watershed characteristics and the generation of runoff and sediment loss in the watershed. In the Gumara-Maksegnit watershed (56 km²), located in the Lake Tana Basin, Amhara, Ethiopia, various field experiments were carried out to investigate different effects of soil and water conservation (SWC) structures at the field level. Objective of this master thesis is the establishment of a calibrated SWAT model in order to be used for up-scaling of SWC impacts to gain a deeper insight into SWC interactions at sub-watershed level related to hydrological and land degradation issues. The study area are two small sub-watersheds of the Gumara-Maksegnit watershed. They are located close to each other with an area of 31 and 41 ha, respectively. 80 % of the area is steeper than 10 %. In one sub-watershed SWC measures (mainly stone bunds) were implemented in 2011 whereas the other watershed remains as an untreated reference. Mean annual precipitation is about 1200 mm from which approximately 90 % rains between June and September. Soil textures range from clay loam to clay. Land use of both watersheds is similar with approximately 60 % of agricultural land. Main crops grown are sorghum, teff, sorghum, faba bean, barley, wheat and chickpea. Since 2011, an automatic weather station is installed as well as weirs are installed at the sub-catchments' outlets to measure runoff. For each erosive event manual samples are taken in addition to a turbidity sensor to monitor sediment yield. The SWAT model calibration was performed using daily based runoff and sediment yield data recorded during rainy season in 2012 with the help of SWAT-CUP. The results for runoff show acceptable to satisfying performance on a daily basis. The Nash-Sutcliffe Efficiency (NSE) is 0.39 and 0.04 for the untreated and treated sub-watershed respectively. Although the model shows an unacceptable soil loss fit on a daily basis it shows satisfying results on a seasonal basis with a simulated mean annual soil loss rate for 2006-2012 of 37.8 t/ha and 32.4 t/ha for the untreated and the treated sub-catchment respectively.

Zusammenfassung

Im Äthiopischen Hochland ist Bodendegradation eines der Kernprobleme. Abholzung führt zu verstärkter Bodenerosion während der Regenzeit. Die damit einhergehende Grabenbildung, wodurch ein schnelle Entwässerung des Einzugsgebietes ermöglicht wird, verändert somit die hydrologischen Eigenschaften eines Einzugsgebietes. Hydrologische Modelle können uns dabei helfen eine Verbindung zwischen lokalen Einzugsgebietseigenschaften und der Entstehung von Abfluss und Erosion herzustellen. Im Gumara-Maksegnit Einzugsgebiet (56 km²), welches sich im Becken des Tanasees in der Amhara Region in Äthiopien befindet, wurden schon viele Feldexperimente durchgeführt um Boden- und Wasserschutzmaßnahmen (BWS) zu evaluieren. Die Aufgabe dieser Masterarbeit ist es ein kalibriertes SWAT-Modell zu erstellen, um anhand dessen, Erkenntnisse betreffend der BWS-Maßnahmen auf andere Gebiete bzw. auf einen größeren Maßstab umlegen zu können. Das Untersuchungsgebiet besteht aus zwei benachbarten Sub-Einzugsgebieten des Gumara-Meksegnit Einzugsgebietes mit einer Fläche von 31 bzw. 41 ha. 80 % der Fläche ist steiler als 10 %. Eines der beiden Sub-Einzugsgebiete (Ayaye) ist mit BWS-Maßnahmen behandelt worden, wobei das zweite als Referenz dient (Aba-Kaloye). Der durchschnittliche Jahresniederschlag beträgt ca. 1200 mm wovon ca. 90 % zwischen Juni und September auftreten. Die Bodentexturen reichen von tonig-lehmig bis lehmig. 60 % der Fläche wird landwirtschaftlich genutzt. Hauptsächlich werden Teff, Puffbohne, Gerste, Weizen, Sorghumhirse und Kichererbse angebaut. Seit 2011 sind im Untersuchungsgebiet eine automatische Wetterstation und je eine Messwehr, wo Wasserspiegel und Sedimentkonzentration gemessen werden, am Sub-Einzugsgebietsauslass installiert. Die Kalibrierung vom SWAT-Modell mittels SWAT-CUP erfolge auf Basis der tagesbasierten Abfluss- und Sedimentdaten, welche während der Regenzeit 2012 aufgezeichnet wurden. Die Kalibrierung für den Abfluss zeigt akzeptable bis zufriedenstellende Ergebnisse mit einer Nash-Sutcliffe Effizienz (NSE) von 0,39 für das unbehandelte und 0,04 für das behandelte Sub-Einzugsgebiet. Die Kalibrierungsergebnisse mit tagesbasierten Sedimentdaten sind nicht zufriedenstellend. Allerdings können die simulierten Jahresdurchschnittswerte für die Periode 2006-2012 von 37,8 t/ha und 32,4 t/ha als zufriedenstellende Ergebnisse angesehen werden.

Table of Contents

1. Introduction and Objective

The Ethiopian population and economy is highly dependent on the agricultural sector, where 80-85% of the people are employed (Mengistu 2006). Because the linkage between the securing of food and a livelihood to the exploitation of the natural resources base in Ethiopia is inextricably (Dejene 2003), land degradation is such a great threat for the future and it requires great effort and resources to ameliorate (Taddese 2001). Especially in the Ethiopian Highlands deforestation for crop production dramatically increased the vulnerability of the soils for rainfall driven soil erosion (Nyssen et al. 2000). Intensive rainfalls during the rainy season (June to September) threaten the mountainous regions to severe land degradation especially on the steep sloped and unprotected areas (Addis et al. 2013).

This master thesis is conducted within the project called “Community based rainfed watershed management”. The project aims to unlock the agricultural potential of the Amhara region of Ethiopia and improve the livelihoods of the local farmers while reducing vulnerability to climate change through community-based watershed management. The first phase of the project, “Unlocking the potential of rainfed agriculture in Ethiopia for improved rural livelihoods”, started in July 2009 and concluded in November 2012. The ongoing phase 2 of the project, “Reducing land degradation and farmers’ vulnerability to climate change in the highland dry areas of northwestern Ethiopia”, started in July 2013 and will run until June 2016. The project is managed by an international collaboration of International Center for Agricultural Research in the Dry Areas (ICARDA), Amhara Agricultural Research Institute (ARARI), Ethiopian Institute of Agricultural Research (EIAR), Gonder Agricultural Research Center (GARC) and University of Natural Resources and Applied Life Sciences, Vienna (BOKU). It is funded by the Austrian Development Agency (ADA), the CGIAR Research Program on Water, Land and Ecosystems and the CGIAR Research Program on Climate Change, Agriculture and Food Security (ICARDA 2014).

The study area for this master thesis are 2 sub-watersheds, Aba-Kaloye (41 ha) and Ayaye (31 ha), of the Gumara-Maksegnit watershed (56 km²) in the Ethiopian highlands. One of them, the Ayaye sub-watershed, is treated with soil and water conservation (SWC) measures, whereas the other one stays as untreated reference. Various field experiments have been taken out in the Gumara-Maksegnit watershed

as well as in these two sub-watersheds to investigate different effects of SWC structures at the field level.

Objective of this master thesis is the establishment of a calibrated SWAT model for the two sub watersheds. Further the effects of SWC measures in the treated sub-watershed in comparison to the untreated sub-watershed should be evaluated. The findings should then be used for the up-scaling of SWC impacts, to gain a deeper insight into SWC interactions at sub-watershed level related to hydrological and land degradation issues.

1.1 Land Degradation in Ethiopia

Land degradation is defined as “a temporary or permanent decline in the productive capacity of the land, or its potential for environmental management” (Scherr & Yadav 1996).

The major causes for land degradation in Ethiopia are the high population density, the rapid population increase, deforestation, low vegetative cover, unbalanced crop and livestock production and severe soil loss (Taddese 2001; Sonneveld & Keyzer 2003). During dry season wind erosion is severe in arid and semiarid regions whereas in the rainy season water erosion is predominant (Taddese 2001). Especially gully erosion has been identified as the major form of water erosion in the Ethiopian highlands (Tebebu et al. 2010).

Hurni (1988) published a soil degradation map with different severity classes of soil erosion in the Ethiopian highlands. This map is displayed in Figure 1. It can be seen that major parts of Ethiopia are affected by soil degradation. Especially in the Ethiopian highlands in the northern part of the country the situation is alarming.

FAO (1986) estimates that the annual soil loss rates in the Ethiopian highlands reach up to over 200 tons per hectare. Further it is estimated that about half of the highlands land area is significantly eroded and over one-fourth is seriously eroded (FAO 1986).

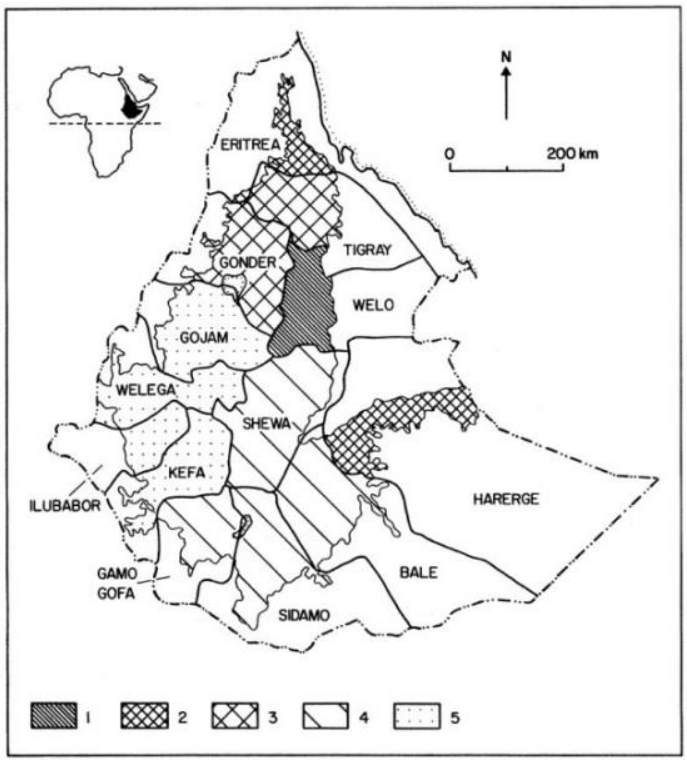

Figure 1: Severity of soil erosion in the Ethiopian highlands: (1) extreme (over 80% of the soils are about 20 cm only deep and the rest about 100 cm); (2) very serious (60-80%); (3) high (40-60%); (4) medium (20-40%); and (5) slight (less than 20%) (Hurni 1988).

Hurni (1988) used the USLE (Wischmeier & Smith 1978) adapted for Ethiopian conditions to estimate annual soil loss rates due to water erosion for the Ethiopian highlands for different land covers. For cropland he estimated an annual soil loss of 42 t/ha, which is significantly higher than the values for grassland, which are 3 to 10 times lower. Soil loss rates exceed soil formation rates by a factor of 4 to 10 for cultivated land and of 0.8 to 2.3 for grassland. It must be mentioned, that these values describe the soil loss of an average land unit, irrespective of the rates of soil accumulation during the process of erosion. Therefore the values do not represent the amount of sediment actually leaving the catchment (Hurni 1988).

Nyssen et al. (2004) developed a formula which describes the relation between the area-specific sediment yield and the drainage area for catchments >1 km².

$$SY = 2595A^{-0.29} \quad (1)$$

where: SY = area-specific sediment yield, in t km^{-2} year^{-1} and A = drainage area, in km².

Further indicative sediment budgets for different catchment sizes were calculated, based on data gained from former studies. While the results suffer from a lack of

spatially distributed data on gully erosion rates they do show however that with increasing catchment size the ratio between deposited sediment within the catchment and total sediment output increases. These results are displayed in Table 1 (Nyssen et al. 2004).

Table 1: Tentative sediment budgets for average catchments of different sizes in the Ethiopian highlands (altered from Nyssen et al. 2004).

Tentative sediment budgets for average catchments of different sizes in the Ethiopian highlands

Catchment size	100 km^2		1000 km^2		10,000 km^2	
	Absolute (t year^{-1})	Specific (t km^{-2} year^{-1})	Absolute (t year^{-1})	Specific (t km^{-2} year^{-1})	Absolute (t year^{-1})	Specific (t km^{-2} year^{-1})
Sources						
Sheet and rill erosion[a]	120,000	1200 (49.1%)	1,200,000	1200 (49.1%)	12,000,000	1200 (49.1%)
Gully erosion[b]	124,000	1240 (50.7%)	1,240,000	1240 (50.7%)	12,400,000	1240 (50.7%)
Dissolution[c]	390	4 (0.2%)	3900	4 (0.2%)	39,000	4 (0.2%)
Total soil loss	244,390	2444 (100%)	2,443,900	2444 (100%)	24,439,000	2444 (100%)
Sinks						
Sediment deposition[d]	175,745	1757 (71.9%)	2,089,944	2090 (85.5%)	22,604,699	2260 (92.5%)
Sediment yield						
Solid sediment loss[e]	68,255	683 (27.9%)	350,056	350 (14.3%)	1,795,301	180 (7.3%)
Dissolved sediment loss[c]	390	4 (0.2%)	3900	4 (0.2%)	39,000	4 (0.2%)
Total catchment sediment output	68,645	686 (28.1%)	353,956	354 (14.5%)	1,834,301	183 (7.5%)

[a] Hurni (1990).
[b] Shibru et al. (2002), Nyssen (2001), De Wit (2003).
[c] Martins and Probst (1991).
[d] (Total soil loss) – (Total catchment sediment output).
[e] Calculated with Eq. (1).

The physical soil loss due to water erosion contributes significantly to the food insecurity situation in Ethiopia and might lead to irreversible changes in soil productivity (Sonneveld & Keyzer 2003). Also Hurni (1988) reports, that it's not by coincidence that the regions with greatest damage due to soil degradation are also the ones most affected by famines. He concludes that soil degradation certainly results in a higher vulnerability to famine (Hurni 1988).

The 1974-1975 famine led to the establishment of a linkage between the degradation of natural resources and famine. Due to this new awareness the Ethiopian government, supported by external aid, made large-scale investments in soil conservation and land rehabilitation measures. The focus was on building physical structures to control soil erosion and to rehabilitate degraded lands (Dejene 2003).

1.2 Soil Erosion

The two main agents causing soil erosion are water and wind. Water erosion is by far the most important type of soil degradation affecting 56 % of the total area suffering

from human-induced soil degradation whereas wind erosion affects 28 % of the total terrain suffering from soil degradation (Oldeman 1992).

1.2.1 Water Erosion

According to Blanco & Lal (2008) water erosion is the “wearing away of the soil surface by water from rain, runoff, snowmelt and irrigation”, while rainwater in the form of runoff is the main driver of water erosion. This definition refers to the movement of soil organic and inorganic particles. The major factors controlling the erosion process are precipitation, vegetative cover, topography and soil properties (Blanco & Lal 2008). In the Universal Soil Loss Equation (USLE) another factor is included, the support practice factor, which takes any soil conservation measures into account (Wischmeier & Smith 1978).

Besides the main on-site effect of erosion, which is the reduction of topsoil thickness, which results in soil structural degradation, soil compaction, nutrient depletion, loss of soil organic matter, poor seedling emergence and reduction of crop yields, there are also several off-site effects. Some of these are the alteration of landscape characteristics, the reduction of wildlife habitat, the damaging of water reservoirs, the pollution, sedimentation and silting of water resources and the accumulation of eroded materials in alluvial plains which might cause inundation of downstream croplands and water reservoirs (Blanco & Lal 2008).

Blanco & Lal (2008) define 6 main types of soil erosion which are splash, interrill/sheet, rill, gully, streambank and tunnel erosion.

1.2.1.1 Splash Erosion

The force of impacting raindrops splashes the soil, causing displacement of particles from their original position. Raindrops form small craters which’s depth is a function of raindrop velocity, size and shape (Blanco & Lal 2008).

1.2.1.2 Interrill/Sheet Erosion

It takes place in between rills, which are developing as soon as runoff starts. Interrill erosion is mostly due to shallow flow and it is the most common type of soil erosion. Splash and interrill erosion make up about 70% of total soil erosion. It is a function of particle detachment, rain fall intensity and field slope (Blanco & Lal 2008).

1.2.1.3 Rill Erosion

It takes place in small channels or rills and occurs due to concentrated flow, which erodes soil at faster rates than interrill erosion. Although the rills can easily be eliminated by tillage operations, intense rains can lead to large soil erosion. Rill erosion is a function of soil erodibility, runoff transport capacity and hydraulic shear of water flow (Blanco & Lal 2008).

1.2.1.4 Gully Erosion

Gullies are defined as either V- or U-shaped channels of at least 0.3m width and 0.3m depth. They are primarily formed by concentrated runoff converging in lower points of the fields. Continued gully erosion removes entire soil profiles. There are two types of gullies:

- Ephemeral gullies: Ephemeral gullies are shallow channels that can be readily corrected by routine tillage operations.
- Permanent gullies: Permanent gullies refer to channels which are too large to be obliterated by normal tillage and require expensive measures of reclamation and control.

The main factors affecting gully erosion are the shear stress of flowing water and the critical shear stress of the soil, which is a function of soil texture, bulk density, clay content, dispersion ratio, tillage, plant roots, residue cover and soil slope (Blanco & Lal 2008).

1.2.1.5 Tunnel Erosion

Tunnels develop due to runoff infiltrating into subsoil layers which are dispersible. When tunnels expand to the point where they no longer support the surface weight, they collapse and form gullies (Blanco & Lal 2008).

1.2.1.6 Streambank Erosion

It describes the bank collapse along streams due to erosive forces of runoff from uplands fields (Blanco & Lal 2008).

1.2.2 Wind Erosion

Wind erosion occurs when the force of wind exceeds the resistance forces of the soil. It is a function of wind intensity, precipitation, surface roughness, soil texture and

aggregation, agricultural activities, vegetation cover and field size (Blanco & Lal 2008).

2. Materials and Methods

2.1 Study Area

The study area, the Aba-Kaloye and the Ayaye sub-watershed, lies within the Gumara-Maksegnit watershed, which is situated in the Lake Tana basin in the northwest Amhara region of Ethiopia (Figure 2). The watershed is dominated by its mountainous topography with steep slopes and ranges from about 1920 m.a.s.l. to 2860 m.a.s.l. in altitude. It covers an area of 54 km² and is located between 12°24' and 12°31' North and between 37°33' and 37°37' East. The watershed drains into the Gumara River, which finally reaches Lake Tana (Addis et al. 2013).

Figure 2: Map locating the study area (Addis et al. 2013).

The two sub-catchments are located in the southern, lower part of Gumara-Maksegnit watershed between 12°25'26'' and 12°25'46'' North and between 37°34'56'' and 37°35'38'' East (Figure 3). They are neighboring each other with a distance of about 1 km between the outlets (Figure 4). Aba-Kaloye and Ayaye sub-watershed embrace an area of 36 ha (Kluibenschädl 2014) and 24 ha respectively while their altitude reaches from about 2000 m.a.s.l. to about 2150 m.a.s.l.

(Zehetbauer 2014). They are also characterized by a mountainous topography with steep slopes, where about 80 % of the area have an inclination >10 %.

Figure 3: Overview of the Gumara-Maksegnit watershed with the location of the two sub-catchment outlets (altered from Addis et al., 2013).

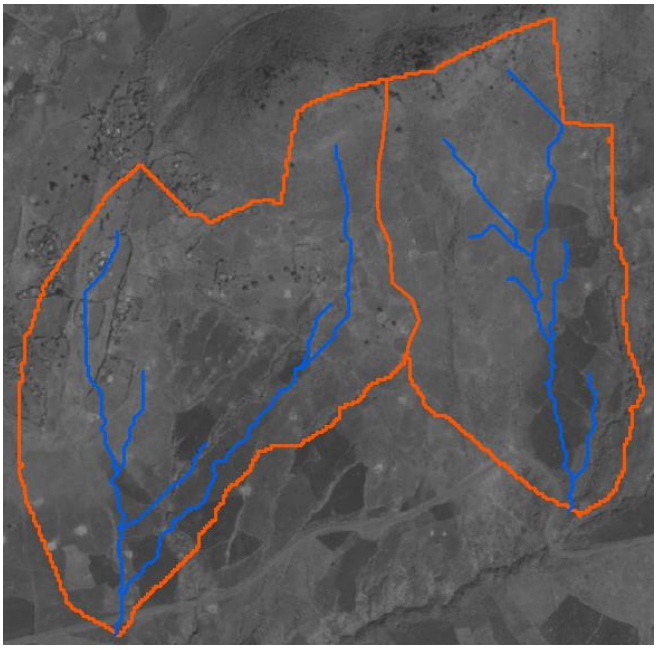

Figure 4: Detailed view of the sub-catchments, with Aba-Kaloye on the left and Ayaye on the right side. Boundaries and delineation are according to the SWAT model based on the DEM. The boundary between the two sub-watersheds was generated manually.

The Aba-Kaloye as well as the Ayaye sub-catchment is involved in long-term soil erosion studies. Both sub-catchments show severe soil erosion problems, which show itself in the development of deep gullies. While in the Ayaye sub-watershed water and soil conservation measures were applied, as the construction of gabions within the gullies and the implementation of stone bunds, the Aba-Kaloye sub-watershed acts as a reference for gully development without measures (Figure 5). In the Ayaye sub-catchment all fields at the west flake are treated with stone bunds except for the fields most to the south (Figure 6) (Brenner 2013). According to Bosshart (1997), the potential short-term benefits of stone bunds are the reduction of slope length and the creation of small retention basins for runoff and sediment. These effects appear immediately after the construction of the stone bunds and result in reduced soil loss. The major medium and long-term effect is the reduction in slope steepness by progressive formation of terraces through the filling up of the retention spaces with sediment.

Figure 5: Gully formation at Aba-Kaloye sub-catchment (Kluibenschädl 2014).

Figure 6: Stone bunds at Ayaye sub-catchment (Zehetbauer 2014).

There exist diverse agroclimatic zones in Ethiopia. Traditionally there are 5 major agroclimatic zones which are shown in Table 2. The Gumara-Maksegnit watershed finds itself in the cool sub-humid agroclimatic zone called Weyna Dega (Dejene 2003).

Table 2: Traditional Agroclimatic Zones of Ethiopia (Dejene 2003).

Zone	Altitude (metres)	Rainfall (mm/year)	Length of Growing Period (days)	Average Annual temperature (°C)
Wurch (cold and moist)	3200 plus	900 – 2200	211 – 365	>11.5
Dega (cool and humid)	2300 – 3200	900 – 1200	121 – 210	17.5/16.0 – 11.5
Weyna Dega (cool sub-humid)	1500 – 2300/2400	800 – 1200	91 – 120	20.0 – 17.5/16.0
Kola (warm semi-arid)	500 – 1500/1800	200 – 800	46 – 90	27.5 – 20
Berha (hot arid)	under 500	under 200	0 – 45	>27.5

Addis et al. (2013) report a mean annual rainfall in the study area of about 1170 mm. More than 90 % occurs during the rainy season. The average monthly maximum

temperature reaches 28.5 °C, whereas the average monthly minimum temperature goes down to 13.6 °C (Addis et al. 2013).

GARC (2010) reports an mean annual rainfall of 1052 mm recorded from 1987 to 2007, whereas the total annual rainfall varies from 641 mm to 1678 mm. Monthly rainfall in the main growing period from May to October ranges from 40.2 mm to 306.1 mm (GARC 2010).

Five different soil textural classes have been determined in the Gumara-Maksegnit watershed: sandy clay loam, sandy loam, clay loam, loam and clay. In the upper part of the watershed shallow loam soils with rooting depth <0.15 m have been found, while in the lower areas of the catchment clay soils with rooting depth >1 m are predominant (Addis et al. 2013). Figure 7 shows the distribution of the different soil textural classes within the watershed. The soil types of the Gumara-Maksegnit watershed are Cambisol and Leptosol in the upper and central part and Vertisol in the lower part of the catchment (Addis et al. unpublished).

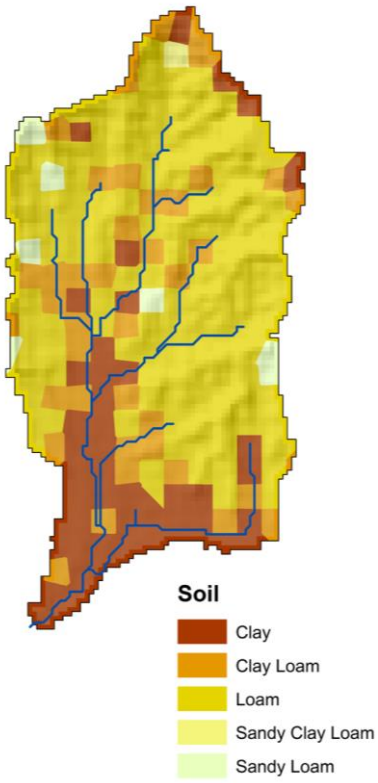

Figure 7: Soil types determined within the Gumara-Maksegnit watershed (Addis et al. 2013).

Within the two sub-catchments, Aba-Kaloye and Ayaye, the determined soil depth (>0.15 m to 1 m) correlates with the soil depth distribution within the whole watershed. Although the soil texture was found to be clay in the area of the sub-

watershed outlets, the predominant soil textural class in Aba-Kaloye is clay loam, while it is loam in Ayaye (Zehetbauer 2014).

In the Gumara-Maksegnit watershed 74 % of the total area is under agricultural use. The major crops are sorghum, teff, faba bean, lentil, wheat, chick pea, linseed, fenugreek and barley, whereas teff and sorghum are the main staple crops while chickpea can only be grown in the lower regions. 23 % of the total watersheds' area is covered by forest, while 2 % are left to pasture land and houses (Addis et al. 2013). Figure 8 shows the distribution of agricultural land, forest and grassland within the Gumara-Maksegnit watershed.

In the sub-catchments 61 % of the combined area is covered by agricultural land. The crops which are grown are teff, sorghum, wheat, chickpea, faba beans and barley. 23 % of the area is occupied by pasture, whereas 16 % is covered by open shrub land. Figure 9 shows the distribution of the land use in the two sub-watersheds.

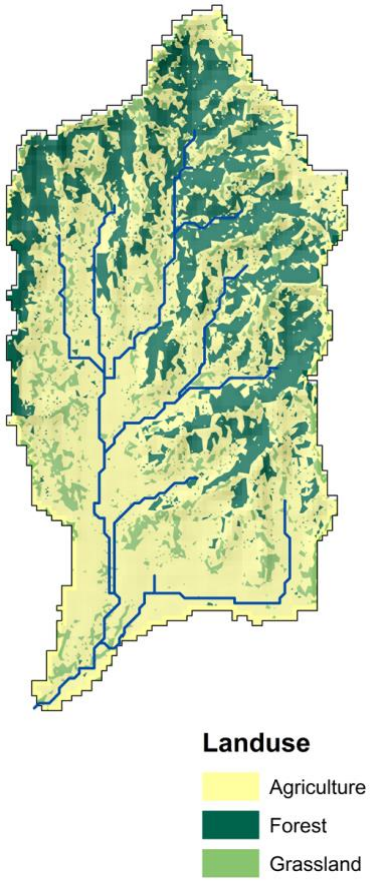

Figure 8: Landuse within the Gumara-Maksegnit watershed (Addis et al. 2013).

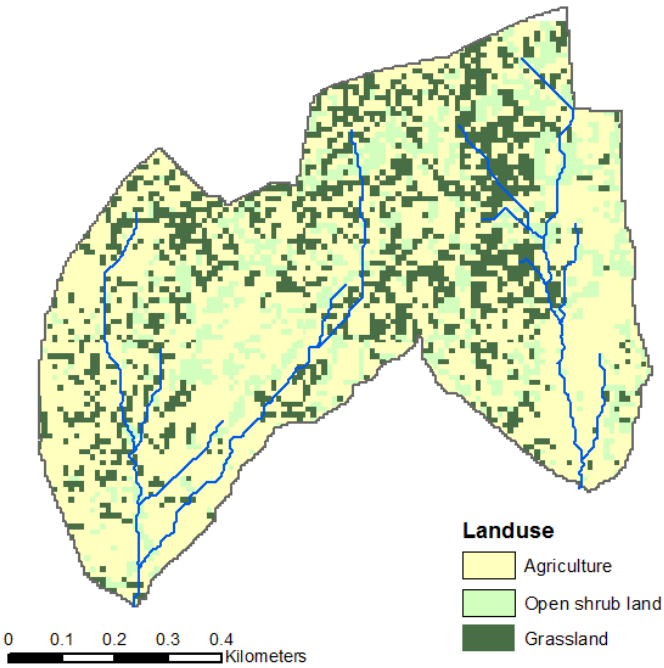

Figure 9: Landuse within the two sub-catchments, Aba-Kaloye and Ayaye.

2.2 SWAT - Soil and Water Assessment Tool

2.2.1 Introduction

The Soil and Water Assessment Tool is a public domain computer program which was developed by Dr. Jeff Arnold for the USDA Agricultural Research Service (ARS). It is a watershed scale model and was developed to predict the impact of land management practices on water, sediment and agricultural chemical yields in large complex watersheds with varying soils, land use and management conditions over long periods of time. Various characteristics are incorporated in the model to be able to satisfy these objectives (Neitsch et al. 2011).

- The model is physically based. SWAT requires specific information about weather, soil properties, topography, vegetation and land management practices in the watershed to directly model the processes like e.g. water movement, sediment transport, crop growth, nutrient cycling. The advantages of a physically based approach are that watersheds with no monitoring can be modeled and that the relative impact of alternative input date can be investigated.
- The minimum data required to make a run is readily available from e.g. government agencies.
- SWAT is computationally efficient, which means that simulations of very large basins or a variety of management strategies can be performed without excessive investment of time and money.
- The model allows users to investigate long-term impacts with runs spanning several decades (Neitsch et al. 2011).

As SWAT is a continuous time model, it is not designed to simulate detailed, single-event flood routing (Neitsch et al. 2011).

2.2.2 Development of SWAT

SWAT is a direct outcome of the merging of two existing models: The SWRRB model (Simulator for Water Resources in Rural Basins) (Williams et al. 1985) and the ROTO model (Routing Outputs to the Outlet) (Arnold et al. 1995) (Neitsch et al. 2011). The SWRRB model is a physically based, continuous time-step model, which was developed for simulating hydrologic and related processes in rural basins (Williams et al. 1985). The ROTO model was developed to overcome the spatial limitations of the

agricultural-management models at that time and to estimate water and sediment yield on large basins (Arnold et al. 1995). SWAT incorporates the benefits of the two models. While allowing simulations on a very large scale, it retained all the features which made SWRRB such a valuable simulation (Neitsch et al. 2011).

Other specific ARS models which contributed to the development of SWAT were CREAMS (Chemicals, Runoff and Erosion from Agricultural Management Systems) (Knisel 1980), GLEAMS (Groundwater Loading Effects on Agricultural Management Systems) (Leonard et al. 1987) and EPIC (Erosion-Productivity Impact Calculator) (Williams et al. 1984) (Neitsch et al. 2011).

Since SWAT was created in the early 1990s, it has undergone continued review and expansion of functions and capabilities. The current version is SWAT2012 which also was used for this project. Interfaces for the model have been developed in Windows (Visual Basic), GRASS and ArcView (Neitsch et al. 2011).

2.2.3 Model Components

SWAT is capable of simulating numerous different physical processes in the watershed. For modeling purposes the watershed is divided in subbasins, which is particularly helpful when the soils or land uses within one watershed are different in a high degree, which might lead to different impact on hydrology. Input information for each subbasin is grouped into the following categories: climate, hydrologic response units (HRUs), ponds/wetlands, groundwater and the main channel/reach draining the subbasin. HRUs are land areas including a certain combination of land cover, soil and slope within one subbasin (Neitsch et al. 2011).

Every simulation with SWAT is based on the water balance within the watershed. The hydrologic cycle within a watershed can be separated into two major divisions: The land phase of the hydrologic cycle, which controls the amount of water, sediment, nutrient and pesticide loadings going into the main reach of each subbasin and the water routing phase, which describes the movement of water, sediments, nutrient and pesticide loadings through the channel network to the outlet of the watershed (Neitsch et al. 2011).

2.2.3.1 Land Phase of the Hydrologic Cycle

SWAT simulates the hydrologic cycle based on the water balance equation:

$$SW_t = SW_0 + \sum_{i=1}^{t}(R_{day} - Q_{surf} - E_a - w_{seep} - Q_{gw}) \quad (2)$$

where SW_t is the final soil water content (mm H_2O), SW_0 is the initial soil water content on day i (mm H_2O), t is the time (days), R_{day} is the amount of precipitation on day i (mm H_2O), Q_{surf} is the amount of surface runoff on day i (mm H_2O), E_a is the amount of evapotranspiration on day i (mm H_2O), w_{seep} is the amount of water entering the vadose zone from the soil profile on day i (mm H_2O) and Q_{gw} is the amount of return flow on day i (mm H_2O) (Neitsch et al. 2011).

A schematic representation of the hydrologic cycle is shown in Figure 10.

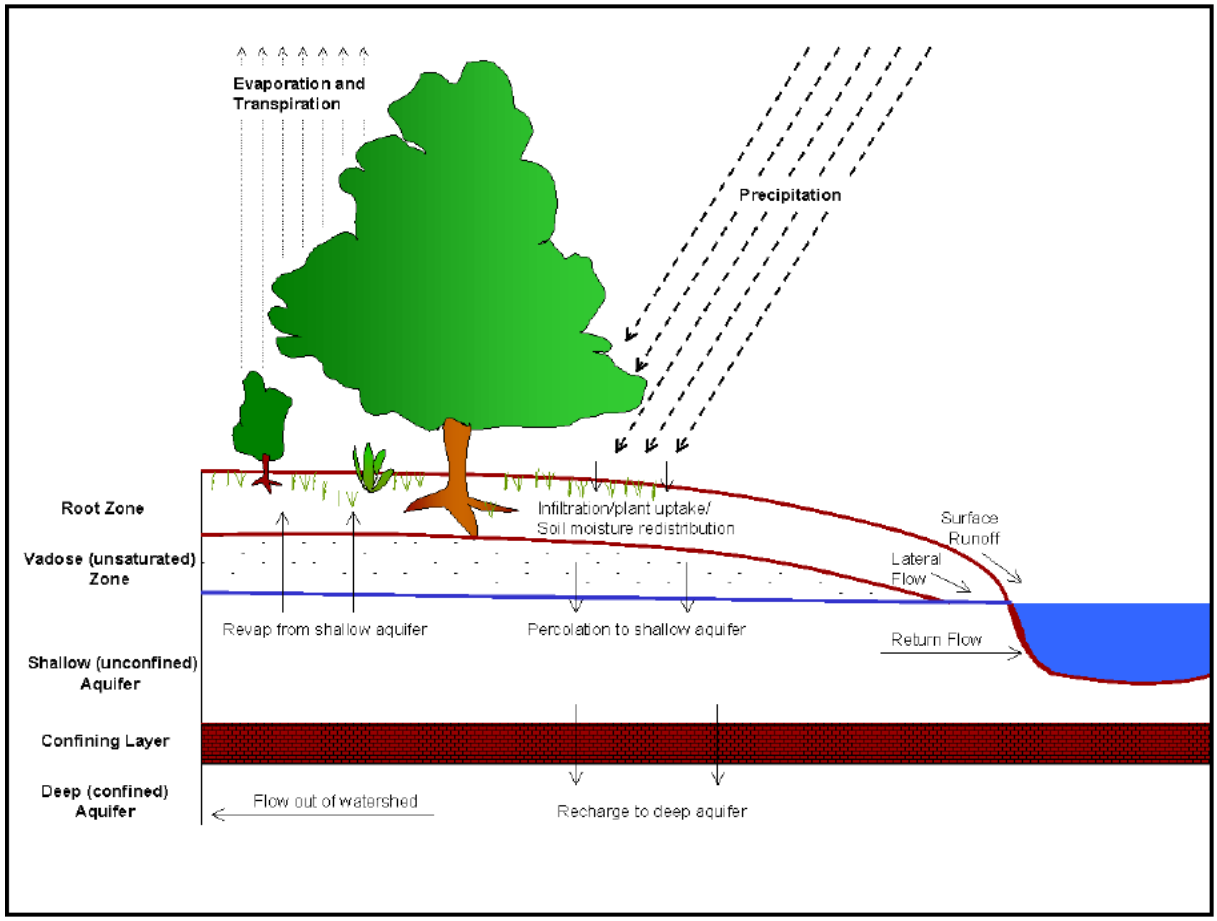

Figure 10: Schematic representation of the hydrologic cycle (Neitsch et al. 2011).

The subdivision into HRUs allows the model to take differences in evapotranspiration for various crops and soils into account and it increases the accuracy of the model as runoff is predicted separately for each HRU and routed to obtain the total runoff for the watershed (Neitsch et al. 2011)

Figure 11 represents the general sequence of processes SWAT uses to simulate the land phase of the hydrologic cycle. The different inputs for and components of the land phase of the hydrologic cycle are described in the following section (Neitsch et al. 2011).

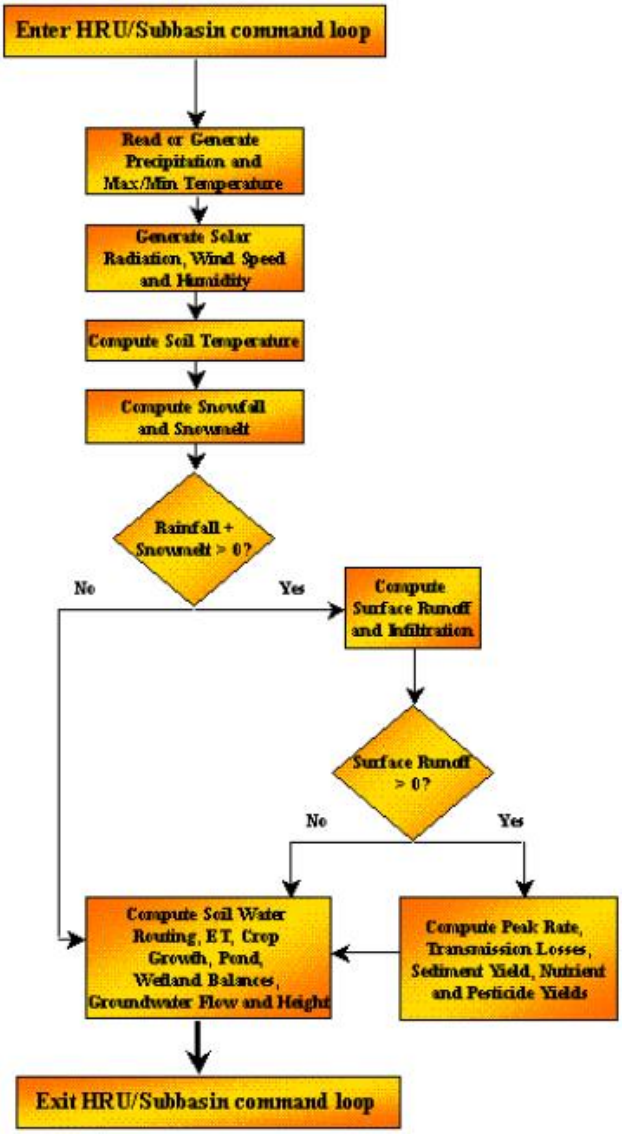

Figure 11: HRU/Subbasin command loop (Neitsch et al. 2011).

2.2.3.1.1 Climate

A watershed's climate is responsible for the moisture and energy inputs that determine the water balance within the watershed. In SWAT the climate is represented by the variables daily precipitation, maximum/minimum air temperature, solar radiation, wind speed and relative humidity. Furthermore a weather generator is implemented in the model to generate daily values from average monthly values and to fill in missing data in the measured records. Snow is also taken into account by SWAT whereas the model classifies precipitation as rain or freezing rain/snow using the average daily temperature. Also the soil temperature is simulated on the surface as well as in the different soil layers (Neitsch et al. 2011).

2.2.3.1.2 Hydrology

SWAT has incorporated many different hydrological components and simulates different hydrological processes. The potential pathways of water movement in SWAT on a HRU scale are depicted in Figure 12.

- Canopy storage: Canopy storage is the water intercepted by vegetative surfaces where it is available for evapotranspiration.
- Infiltration: Infiltration is described as the entry of water into a soil profile from the soil surface. The rate of infiltration decreases with time until it reaches a constant value.
- Redistribution: Redistribution is the continued movement of water through a soil profile after water input has ceased. It is caused by the different distribution of water content in the soil profile.
- Evapotranspiration: Evapotranspiration includes all processes at or near the earth's surface which turn water in the liquid or solid phase into atmospheric water vapor. Further it is distinguished between potential and actual evapotranspiration.
- Lateral subsurface flow: Lateral subsurface flow, or interflow, contributes to streamflow and originates below the surface but above the saturated zone.
- Surface runoff: Surface runoff is flow that occurs along a sloping surface. SWAT simulates surface runoff volumes and peak runoff rates for each HRU.
- Ponds: Ponds are structures located within a subbasin which store water and therefore intercept surface runoff.
- Tributary channels: Tributary channels are besides the main channel one of two types of channels within a subbasin. They are channels of lower order branching off the main channel within the subbasin.
- Return flow: Return flow, or base flow, is the stream flow contributing from groundwater layers. SWAT divides groundwater into two aquifer layers: a shallow, unconfined aquifer and a deep, confined aquifer (Neitsch et al. 2011).

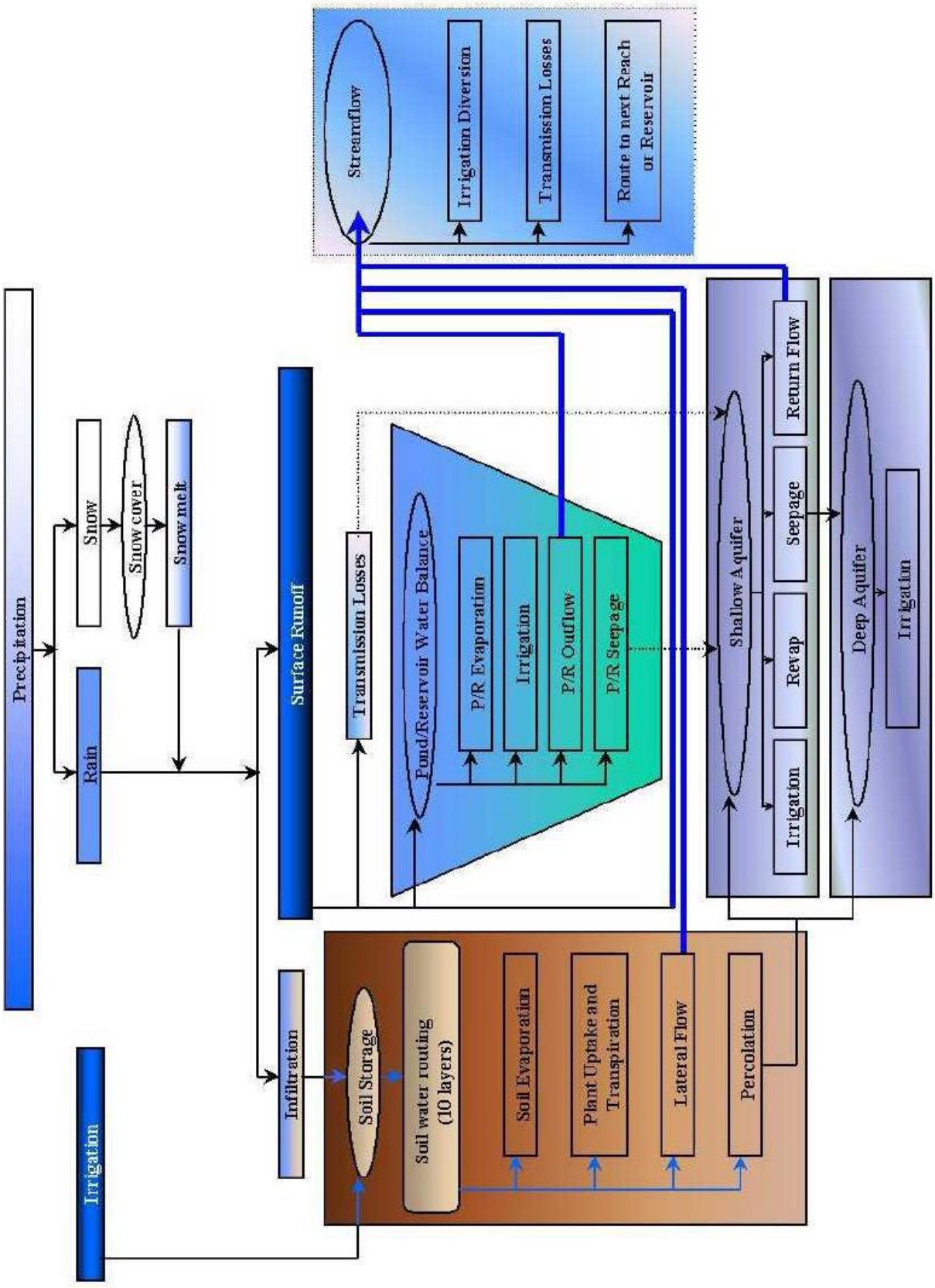

Figure 12: Schematic representation of the potential pathways for water movement in SWAT (Neitsch et al. 2011).

2.2.3.1.3 Land Cover/Plant Growth

In SWAT a single plant growth model is implemented to simulate all types of land covers. It is distinguished between annual and perennial plants. While annual plants grow from the planting date to the harvest date, perennial plants maintain their root systems throughout the year becoming dormant during winter. With the plant growth model the removal of water and nutrients from the root zone, transpiration and biomass/yield production can be assessed easily (Neitsch et al. 2011).

2.2.3.1.4 Erosion

SWAT estimates the erosion and sediment yield for each HRU with the Modified Universal Soil Loss Equation (MUSLE) (Williams, 1975). While the USLE uses rainfall to calculate the erosive energy, MUSLE uses the amount of runoff to simulate erosion and sediment yield. The major benefits of the MUSLE are the prediction accuracy and the possibility of estimating the sediment yields of single storm events (Neitsch et al. 2011).

2.2.3.1.5 Nutrients

SWAT simulates the movement and transformation of several forms of nitrogen and phosphorus in the watershed. In the soil the processes are governed by the nitrogen and by the phosphorus cycle shown in Figure 13 and Figure 14 respectively. Through surface runoff and lateral subsurface flow nutrients may be entering the main channel and therefore be transported downstream (Neitsch et al. 2011).

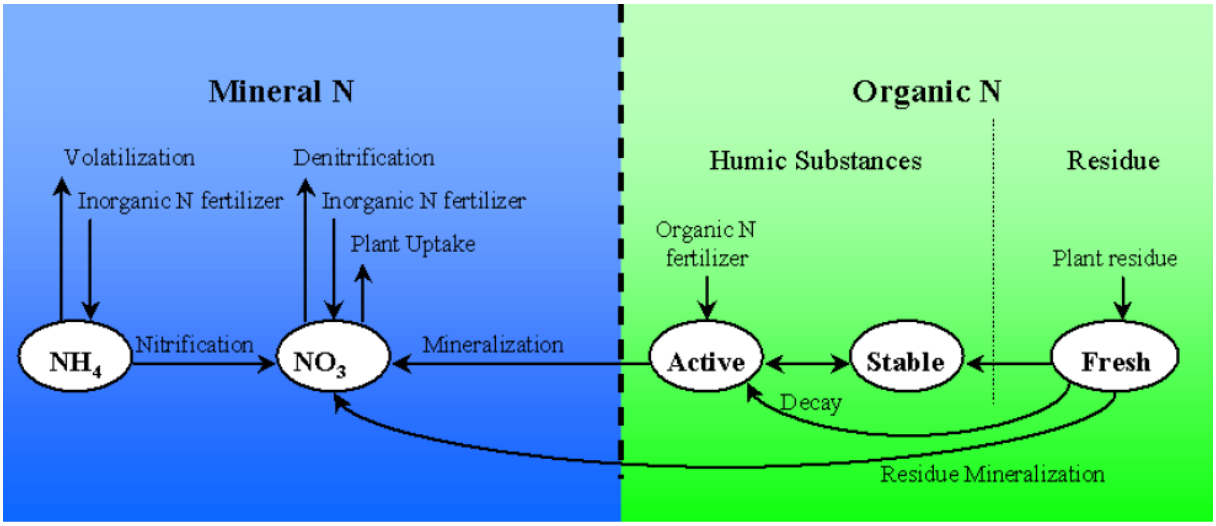

Figure 13: N cycle in SWAT (Neitsch et al. 2011).

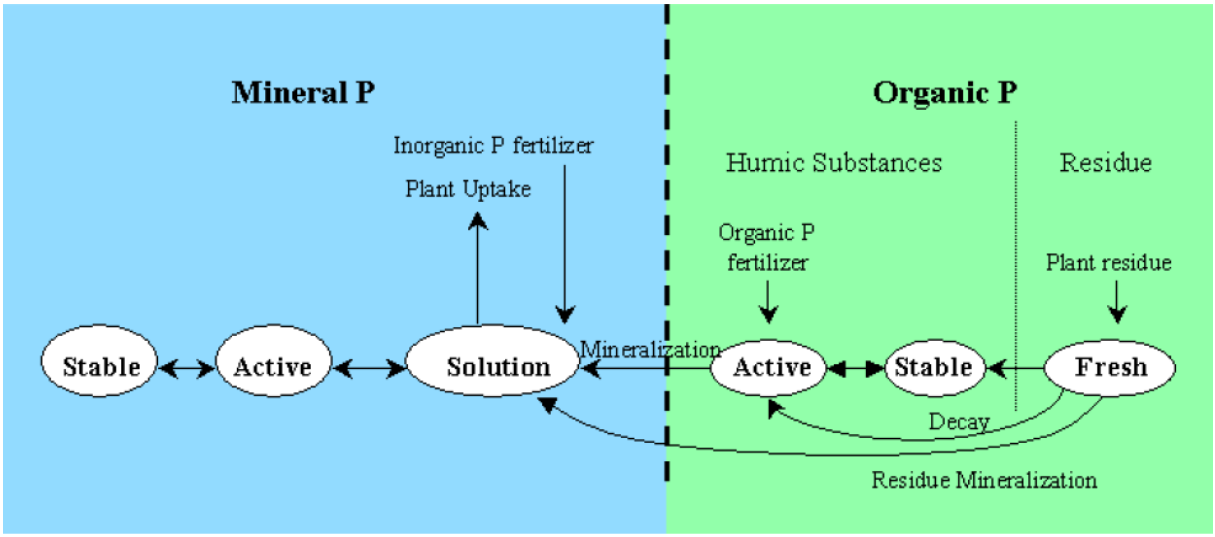

Figure 14: P cycle in SWAT (Neitsch et al. 2011).

2.2.3.1.6 Pesticides

Pesticides can be applied on a HRU scale in SWAT to study the movement of the chemical in the watershed. The pesticide movement is simulated within the stream network as well as within the soil profile (Neitsch et al. 2011).

2.2.3.1.7 Management

The user may define management practices on a HRU scale such as the beginning and ending of the growing season, the timing and amounts of fertilizer, pesticides and irrigation applications and the timing of tillage operations. At the end of growing the user can define either the removal of biomass or the placement on the surface as residue (Neitsch et al. 2011).

2.2.3.2 Routing Phase of the Hydrologic Cycle

After determining the loadings of water, sediment, nutrients and pesticide to the main channel, SWAT routes the loadings through the stream network of the watershed. SWAT model also takes the transformation of chemicals in the stream and streambed into account, in order to monitor the mass flow. All in-stream processes modeled by SWAT are illustrated in Figure 15. Further SWAT distinguishes between two major routing processes: routing the main channel and routing in the reservoir (Neitsch et al. 2011).

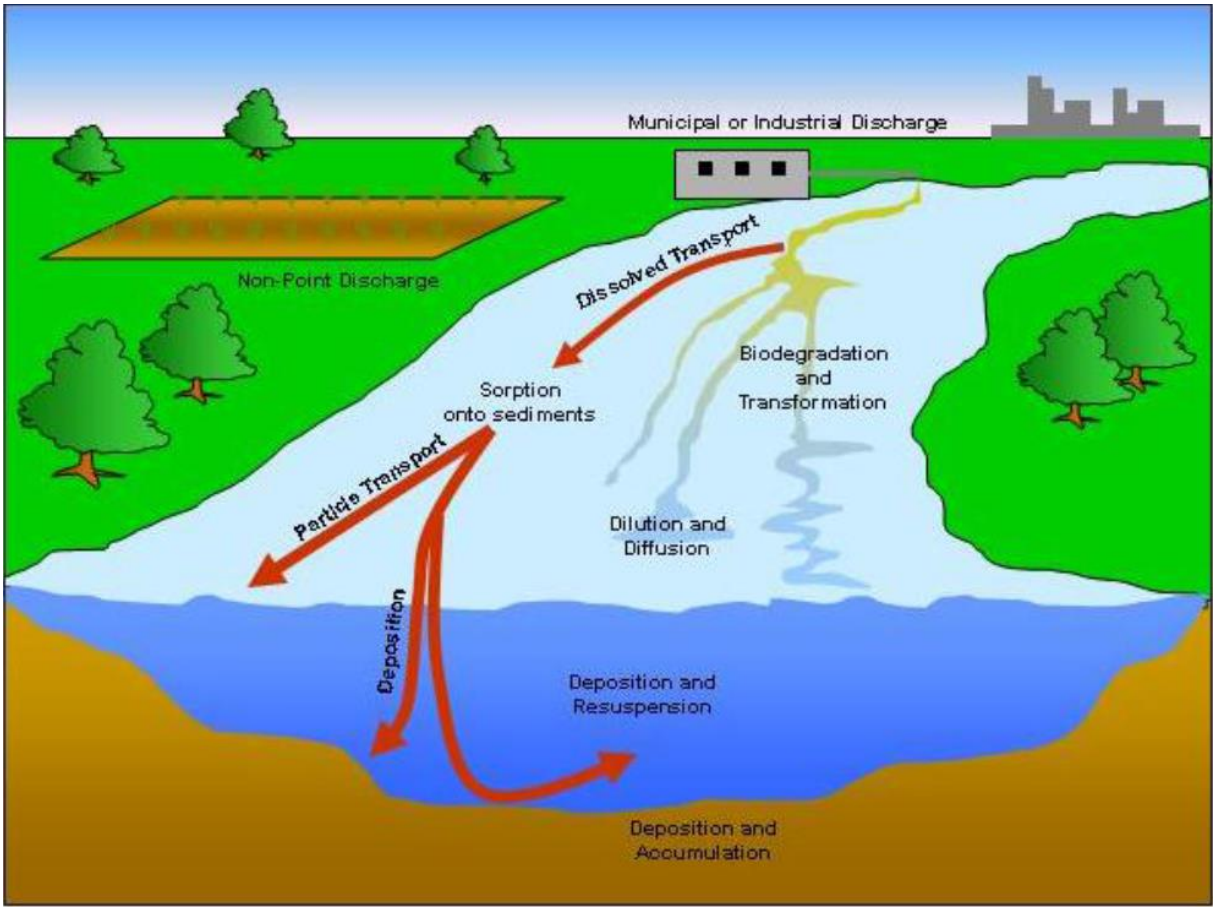

Figure 15: In-stream processes modeled by SWAT (Neitsch et al. 2011).

2.2.3.2.1 Routing in the Main Channel or Reach

Four components describe the routing in the main channel: water, sediment, nutrients and organic chemicals.

- Flood routing: Several processes may influence the mass balance of the water flowing downstream. Losses may appear due to evaporation and transmission through the bed of the channel as well as due to the removal of water for agricultural or anthropogenic use. Flow may be supplemented by rain fall directly on the channel and by point source discharges. SWAT incorporates two methods for flood routing: the variable storage coefficient method (Williams 1969) or the Muskingum routing method.
- Sediment routing: Sediment transport is controlled by two simultaneously occurring processes, deposition and degradation. The maximum amount of sediment possibly transported from a reach segment is a function of the peak channel velocity.

- Nutrient routing: Nutrient transformation processes in the stream are controlled by the in-stream water quality component of SWAT. The model distinguishes between dissolved nutrients and nutrients absorbed to the sediment.
- Channel pesticide routing: Only one pesticide may be routed through the channel network due to the complexity of the simulated processes. Again the model separates the pesticides into dissolved and sediment-attached pesticides (Neitsch et al. 2011).

2.2.3.2.2 Routing in the Reservoir

The water balance for reservoirs includes inflow, outflow, rainfall on the water surface, evaporation and seepage from the reservoir. SWAT routes the outflow, the sediment concentration, the nutrient concentration and the concentration of the reservoir pesticides.

2.3 Additional Software

Besides SWAT2012, SWAT-CUP was used for auto-calibration purposes.

2.3.1 SWAT Calibration and Uncertainty Programs

SWAT Calibration and Uncertainty Programs (SWAT-CUP) is a public domain computer program for the calibration of SWAT models which was developed by the aquatic research institute Eawag located in Switzerland. The program enables sensitivity analysis, calibration, validation and uncertainty analysis of SWAT models. It incorporates different algorithms such as SUFI2, PSO, GLUE, ParaSol and MCMC (Abbaspour 2014). In SWAT-CUP a certain range can be assigned to a chosen set of parameters. SWAT-CUP runs a given number of simulations and changes the parameters within the chosen range to compare the output with the measured data following a certain algorithm.

2.4 Model Input

2.4.1 Rainfall and Temperature Data

Rainfall and temperature data was available from 1997 to 2013. Until the end of 2009 the rain data was monitored at a gauge respectively close to the study area, while starting with the year 2010 the rain data was monitored at a gauge situated within Aba-Kaloye sub-watershed (H.K. Addis 2014, pers. comm., 30 July). Temperature

data was monitored at the same gauges for the same time periods as the rain data (H.K. Addis 2014, pers. comm., 1 Oct.). The analysis of the rain and temperature data showed, that there are data gaps for certain periods in both time series as well as missing data for single rainfall events. The following table (Table 3) shows the time period of missing data for rainfall and temperature data as well as the number of single rainfall events missing.

Table 3: List of missing rainfall and temperature data.

Rainfall data		**Temperature data**	
Time periods of missing data		*Time periods of missing data*	
2003	1.1. – 31.1	2005	1.4. –30.4., 1.9. – 31.12.
2005	1.4. –30.4., 1.9. – 31.12.	2006	1.12. – 31.12.
2007	1.1. – 31.1.	2007	1.1. – 28.2.
2009	1.1. – 28.2., 1.4. – 31.5., 1.8. – 31.8., 1.10. – 31.10.	2009	1.1. – 28.2., 1.4. – 31.5., 1.8. – 31.8., 1.10. – 31.10.
Single rainfall events missing per year (number of missing events in brackets)			
1997(4), 1998(3), 1999(3), 2000(3), 2001(2), 2002(5), 2004(2), 2006(21), 2008(2);			

The missing rainfall and temperature data is generated by SWAT during the modeling process by using the included WXGEN weather generator model (Sharpley & Williams 1990). Depending on the model period the generated values will differ, which leads to a very low reliability for years with big data gaps. The following table (Table 4) shows the annual rainfall from 1997 to 2013 (model period: 1997-2013).

Table 4: Annual rainfall from 1997 to 2013.

Annual rainfall					
Year	*Rainfall (mm)*	*Year*	*Rainfall (mm)*	*Year*	*Rainfall (mm)*
1997	1511	2003	1121	2009	984
1998	1365	2004	942	2010	1119
1999	1620	2005	874	2011	1397
2000	1342	2006	1490	2012	942
2001	1683	2007	1487	*2013*	*2087*
2002	818	2008	1209		

2.4.2 Digital Elevation Model

The digital elevation model (DEM) of the sub-watersheds was generated by using data collected with Theodolites (H.K. Addis 2014, pers. comm., 2 Oct.), resulting in a resolution of about 5.02 m x 5.02 m.

2.4.3 Soil and Land-Use Data

The soil map is based on soil samples taken in a 500 m by 500 m square grid across the entire watershed (Addis et al. unpublished), while the soil map in the sub-watersheds is based on 47 soil samples. As some soil properties such as available water content and hydraulic conductivity for the three layers and bulk density for the second and third soil layers where not measured but are required by the SWAT model, a pedotransfer function developed by Saxton & Rawls (2006) was used to obtain the required soil properties. The land-use data was obtained based on supervised classification of 10 m SPOT satellite image from 2007 using Erdas Imagine 9.1 (Addis et al. unpublished).

2.4.4 Watershed Deliniation

When delineating the watershed in SWAT the drainage area should be set to a value to obtain an even distribution of the subbasins in size within the model area to avoid possible problems in the routing process at subbasin inlets/outlets (R. Srinivasan 2014, pers. comm., 1 Sept.). Kluibenschädl (2014) monitored the gully network in the Aba-Kaloye sub-watershed within the rainy season in 2012. Considering these two aspects the drainage area was set to 1.5 ha.

2.4.5 Management Practices

Tillage practice and planting/harvesting dates were implemented according to information of N. Demelash (2014, pers. comm., 10 Sept.) and GARC (2010). Two crop rotations, which were implemented in the SWAT model, are practiced in the study area in a 3-year rotation: sorghum – chickpea – teff and sorghum – faba bean – barley. Further fertilizer application was taken into account. In the two sub-watersheds teff, barley and wheat are fertilized with urea (N. Demelash 2014, pers. comm., 15 Sept.).

Not all of the crops grown in the study area are included in the SWAT Crop Database. Table 5 shows the land use in reality, the land use chosen in SWAT and the SWAT plant code. For the representation of both chickpeas and faba beans lentils were chosen (R. Srinivasan 2014, pers. comm., 24 Sept.). To keep them each as separate land use throughout the modeling process two different plant codes were used. In the original look up file the plant code used for chickpea and faba beans was LICH and LIMA respectively as at the time the model was set up Chickpea and faba beans were based on data of lima beans. Therefore the plant codes LICH and LIMA

show up as landuse in the SWAT model, whereas the plant codes LECH and LEFA show up in the .mgt file to represent chickpea and faba beans respectively.

Table 5: Information about the implementation of the different land uses in SWAT.

Land use	Land use in SWAT	SWAT plant code
Eragrostis Teff	Eragrostis Teff	TEFF
Sorghum	Grain sorghum	GRSG
Barley	Spring barley	BARL
Open shrub land	Range-brush	RNGB
Grassland	Pasture	PAST
Wheat	Spring wheat	SWHT
Chickpea	Lentils	LICH/LECH (based on LENT)
Faba bean	Lentils	LIMA/LEFA (based on LENT)

2.5 Calibration Data

2.5.1 Crop Data

Guiding values for the annual average crop yield for each of the 6 crops were available (Table 6) (N. Demelash 2014, pers. comm., 15 Sept.).

Table 6: Guideline values for the annual average crop yield in the study area.

	Teff *kg/ha*	**Sorghum** *kg/ha*	**Barley** *kg/ha*	**Wheat** *kg/ha*	**Chickpea** *kg/ha*	**Faba bean** *kg/ha*
Average crop yield	1700	1200	2400	2500	2600	3000

2.5.2 Runoff and Sediment Data

Data of the water level (2011 and 2012) as well as of the sediment concentration (2012) was monitored for both sub-watersheds at the outlet gauging stations. The setup of the measuring devices in 2012 by the example of Aba-Kaloye sub-watershed is depictured in Figure 16.

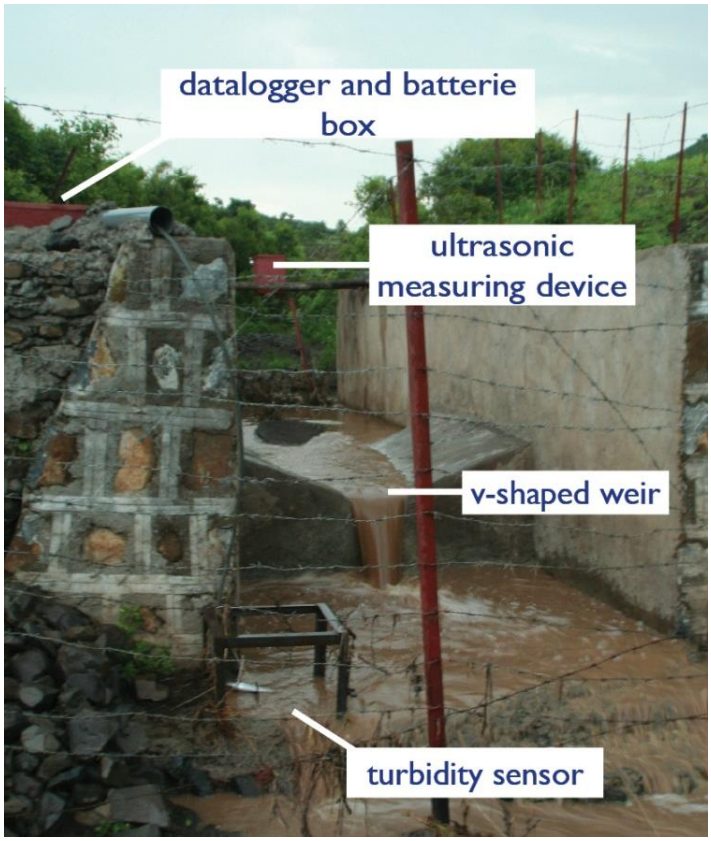

Figure 16: Measuring devices setup in 2012 in Aba-Kaloye sub-watershed. The ultrasonic sensor was used for measuring the water level and the turbidity sensor was used to estimate the sediment concentration (Zehetbauer 2014).

2.5.2.1 Runoff Data

A rating curve was established to transform the data of the water level into runoff (Zehetbauer 2014; Addis et al. unpublished). In 2011 runoff data was collected by staff members of the Gondar Agricultural Research Center and was available from 7.7.2012 to 7.9.2012 for the Aba-Kaloye sub-watershed and from 3.7.2012 to 20.7.2012 for the Ayaye sub-watershed. In 2012 runoff data was collected by Zehetbauer (2014) and was available from 29.6.2012 to 12.8.2012 for the Aba-Kaloye sub-watershed and from 6.7.2012 to 18.8.2012 for the Ayaye sub-watershed. Measurement problems in 2012 led to gaps in the runoff data for both sub-watersheds (Zehetbauer 2014). The following table (Table 7) shows the available runoff data for both sub-watersheds and the according rainfall. Runoff events smaller than 0.15 mm were excluded to eliminate some of the events with the highest uncertainty (Zehetbauer 2014). The runoff in mm is based on the sub-watersheds' area according to the SWAT model.

Table 7: Overview of available runoff data for both sub-watersheds. Area according to the SWAT model.

Aba-Kaloye (41.4 ha, untreated)			
Date	*Rainfall*	*Runoff*	
MM/DD/YYYY	mm	m³/day	mm
7/7/2011	16.6	77.6	0.2
7/12/2011	19.8	199.5	0.5
7/13/2011	24.8	436.3	1.1
7/28/2011	30.2	710.2	1.7
7/30/2011	44.0	1440.4	3.5
8/1/2011	18.4	594.5	1.4
8/2/2011	10.0	435.1	1.1
8/3/2011	20.2	1027.5	2.5
8/7/2011	20.6	831.7	2.0
8/16/2011	15.2	194.6	0.5
8/17/2011	13.4	227.6	0.6
8/21/2011	11.6	145.8	0.4
8/26/2011	15.0	328.7	0.8
8/29/2011	23.6	123.9	0.3
9/4/2011	11.8	434.8	1.1
9/15/2011	18.2	230.0	0.6
7/6/2012	11.4	76.2	0.2
7/7/2012	38.8	1107.5	2.7
7/8/2012	30.8	1704.0	4.1
7/9/2012	14.0	420.2	1.0
7/11/2012	19.0	967.1	2.3
7/16/2012	11.8	110.5	0.3
7/17/2012	9.8	207.2	0.5
7/18/2012	18.0	411.0	1.0
7/19/2012	21.8	1352.3	3.3
7/20/2012	16.4	1303.6	3.2
7/21/2012	12.2	804.8	1.9
7/24/2012	30.2	2600.9	6.3
7/25/2012	14.4	521.8	1.3
7/27/2012	32.2	2370.5	5.7
7/28/2012	21.6	1111.0	2.7
8/2/2012	32.0	1273.3	3.1
8/12/2012	15.4	1130.7	2.7

Ayaye (30.5 ha, treated)			
Date	*Rainfall*	*Runoff*	
MM/DD/YYYY	mm	m³/day	mm
7/7/2011	16.6	85.2	0.3
7/12/2011	19.8	170.3	0.6
7/13/2011	24.8	446.5	1.5
7/28/2011	30.2	77.5	0.3
7/30/2011	44.0	595.8	2.0
8/1/2011	18.4	267.2	0.9
8/2/2011	10.0	321.6	1.1
8/3/2011	20.2	837.8	2.7
8/7/2011	20.6	752.8	2.5
8/16/2011	15.2	90.6	0.3
8/17/2011	13.4	208.4	0.7
8/19/2011	7.4	106.9	0.3
8/21/2011	11.6	190.9	0.6
8/26/2011	15.0	316.3	1.0
8/29/2011	23.6	74.7	0.2
9/4/2011	11.8	297.8	1.0
9/15/2011	18.2	235.4	0.8
7/7/2012	38.8	310.2	1.0
7/8/2012	30.8	684.6	2.2
7/9/2012	14.0	222.4	0.7
7/11/2012	19.0	449.2	1.5
7/17/2012	9.8	215.9	0.7
7/18/2012	18.0	407.8	1.3
7/19/2012	21.8	826.5	2.7
7/20/2012	16.4	635.0	2.1
7/21/2012	12.2	389.0	1.3
7/23/2012	17.0	756.6	2.5
7/24/2012	30.2	1097.9	3.6
7/25/2012	14.4	465.6	1.5
7/27/2012	32.2	1442.3	4.7
7/28/2012	21.6	483.4	1.6
8/2/2012	32.0	434.6	1.4
8/3/2012	14.2	284.1	0.9
8/4/2012	6.6	109.1	0.4
8/5/2012	23.2	270.2	0.9
8/12/2012	15.4	701.5	2.3
8/16/2012	*0.2*	*1385.1*	*4.5*
8/17/2012	*29.2*	*669.1*	*2.2*

The last two events on 16.8.2012 and 17.8.2012 in Ayaye sub-watershed were not used for the calibration process due to inconsistency regarding the rainfall data (see also chapter 3.1.1).

Figure 17 and Figure 18 show bar diagrams of the observed runoff for the rainy season in 2011 and 2012 with the according rainfall. By depicturing the data in the form of diagrams it is clearly evident that the underlying data suffers from substantial data gaps. Further the unstable runoff/rainfall ration within one rainy period is remarkable.

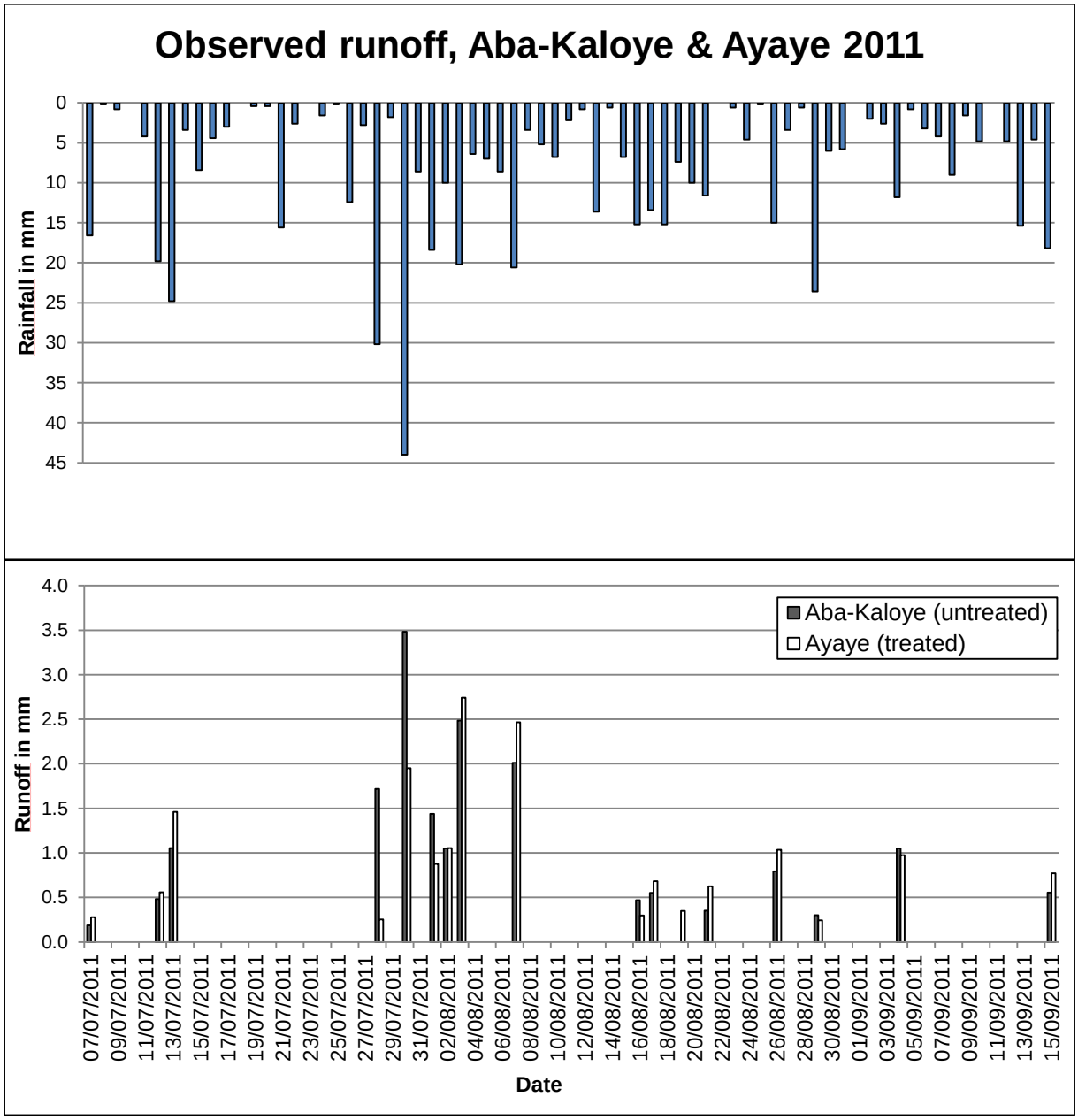

Figure 17: Bar diagram of the observed runoff events in 2011 with the according rainfall event.

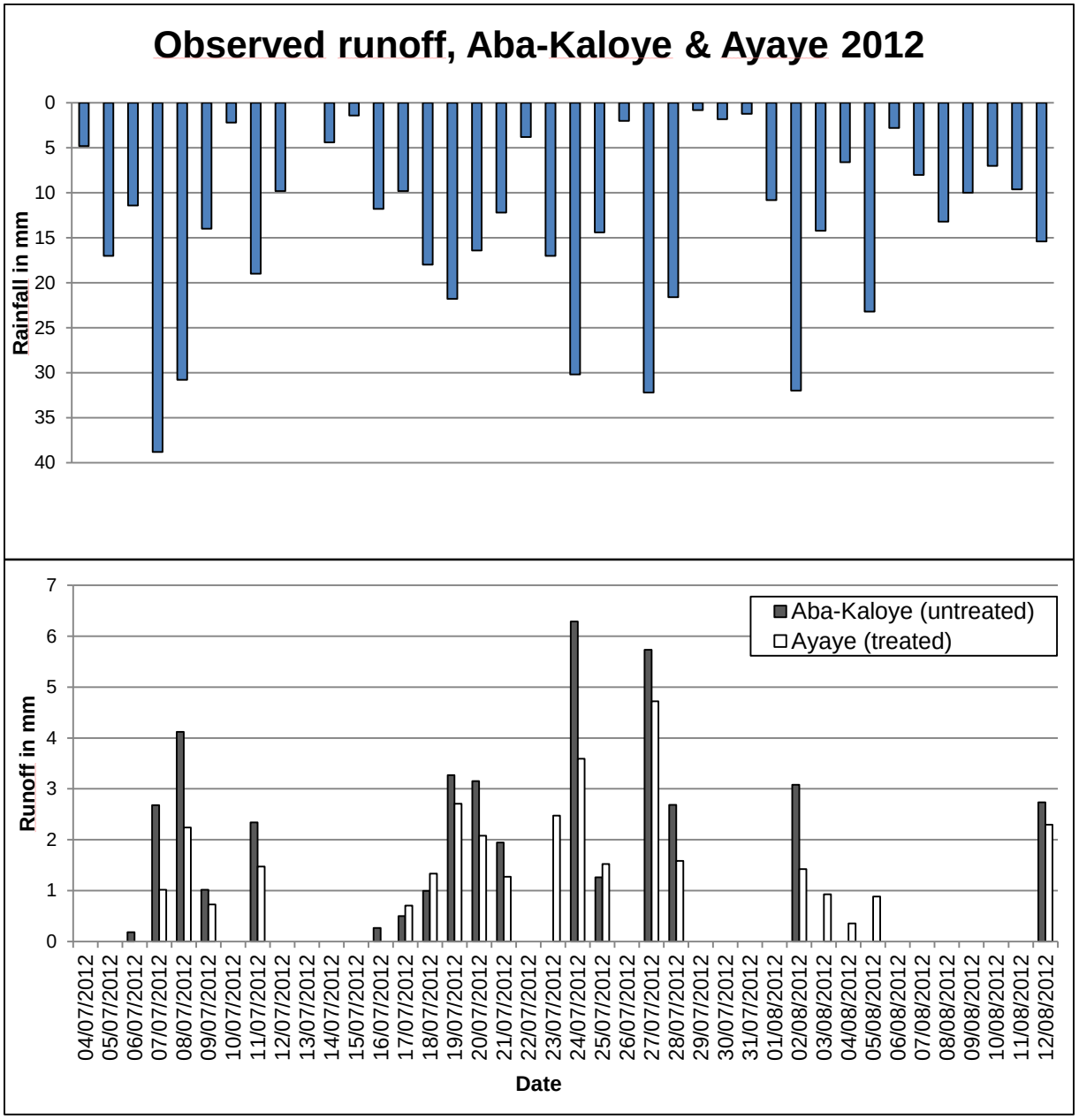

Figure 18: Bar diagram of the observed runoff events in 2012 with the according rainfall event.

A high uncertainty in the monitored data of runoff must be assumed, although no quantitative statements can be made (see also chapter 3.1.2) (Addis et al. unpublished; Zehetbauer 2014).

2.5.2.2 Sediment Data

Data of sediment concentration was available for 2012. It was available from 5.7.2012 to 12.8.2012 for Aba-Kaloye sub-watershed and from 6.7.2012 to 4.8.2012 for Ayaye sub-watershed. Measurement problems led to gaps also in the sediment concentration data for both sub-watersheds (Zehetbauer 2014). The following table (Table 8) shows the available sediment data for both sub-watersheds.

Table 8: Overview of the available sediment data for both sub-watersheds.

Aba-Kaloye (41.4 ha, untreated)				Ayaye (30.5 ha, treated)			
Date	*Rainfall*	*Sediment yield*		*Date*	*Rainfall*	*Sediment yield*	
MM/DD/YYYY	mm	t/day	t/ha	MM/DD/YYYY	mm	t/day	t/ha
7/5/2012	17.0	1.81	0.04	7/6/2012	11.4	0.07	0.00
7/6/2012	11.4	2.26	0.05	7/7/2012	38.8	22.47	0.74
7/7/2012	38.8	27.11	0.66	7/8/2012	30.8	60.62	1.98
7/8/2012	30.8	129.31	3.13	7/9/2012	14.0	10.01	0.33
7/9/2012	14.0	13.60	0.33	7/11/2012	19.0	23.29	0.76
7/11/2012	19.0	45.36	1.10	7/17/2012	9.8	10.95	0.36
7/16/2012	11.8	1.78	0.04	7/18/2012	18.0	14.97	0.49
7/17/2012	9.8	3.47	0.08	7/19/2012	21.8	24.62	0.81
7/18/2012	18.0	7.09	0.17	7/20/2012	16.4	30.86	1.01
7/19/2012	21.8	69.76	1.69	7/21/2012	12.2	23.47	0.77
7/20/2012	16.4	31.86	0.77	7/24/2012	30.2	54.75	1.79
7/21/2012	12.2	15.81	0.38	8/2/2012	32.0	7.20	0.24
7/27/2012	32.2	55.37	1.34	8/3/2012	14.2	9.88	0.32
7/28/2012	21.6	16.94	0.41	8/4/2012	6.6	1.94	0.06
8/12/2012	15.4	18.01	0.44				

Figure 19 shows a bar diagram of the observed sediment data for the rainy season 2012 with the according rainfall. Again it is evident that the underlying sediment data suffers from considerable gaps of missing data. Further the ratio of sediment yield to rainfall on 7.7.2012 compared to 8.7.2012 is remarkable. On 7.7.2012 38.8 mm of rainfall lead to 0.66 t/ha (Aba-Kaloye) and 0.74 t/ha (Ayaye) of sediment yield. However, on 8.7.2012 30.8 mm of rainfall lead to 3.13 t/ha (Aba-Kaloye) and 1.98 t/ha (Ayaye) of sediment yield. A possible explanation could be that sub-daily processes govern the hydrological behavior within the sub-watersheds which cannot be captured by data on a daily time step, like bank failure due to the remaining pore water pressure after water level drawdown after a flood (Lawler et al., 1997) or the intensity of rainfall, which is only simulated with the help of the WXGEN weather generator model (Sharpley & Williams 1990) and therefore a source of uncertainty. Also temporal different infiltration capacities of the soil could lead to such a behavior. Of course, another possible explanation could be a mere measurement error.

Again a high uncertainty in the monitored data of sediment concentration must be assumed, although no quantitative statements can be made (see also chapter 3.1.2) (Addis et al. unpublished; Zehetbauer 2014).

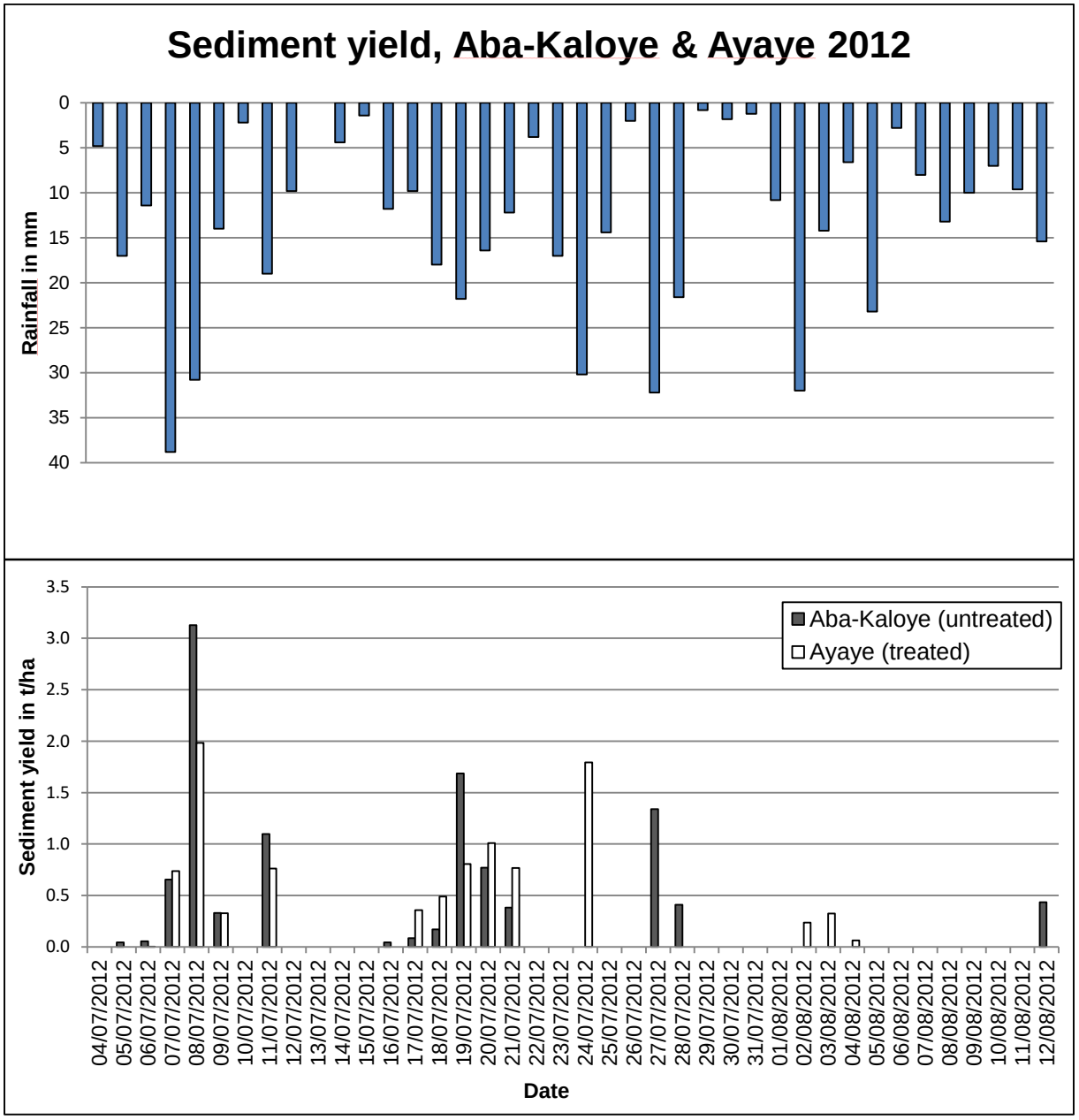

Figure 19: Bar diagram of the observed sediment yield events in 2012 with the according rainfall event.

2.6 Calibration

According to Moriasi et al. (2007) model calibration is the process of estimating model parameters by comparing model predictions (output) for a given set of assumed conditions with observed data for the same conditions. Manual calibration as well as SWAT CUP was used during the calibration process. Due to the data scarcity model validation was not possible.

The indicative values of the average crop yield of each crop were used for manual calibration, by adjusting the Heat Units to maturity of chickpea and faba beans as well as the amount of applied fertilizer (FRT_KG.mgt) for teff, barley and wheat.

For simulating the soil conservation effects of stone bunds in the Ayaye sub-watershed practice factor and curve number were adjusted for the agricultural HRU's (R. Srinivasan 2014, pers. comm., 28 Oct.). Erosion plots in the study area in 2012 showed that stone bunds had a minor soil conservation effect with a P-factor ranging from 1 to 0.66 (Addis et al. unpublished). Comparing the observed sediment loss in the untreated Aba-Kaloye and in the treated Ayaye sub-watershed on days where measured data exists for both sub-watersheds showed a ratio of about 0.87. Therefore it was decided to set the practice factor (USLE_P.mgt) to 0.85. Further the curve number (CN2.mgt) was reduced by 10% to simulate the retention effect of the stone bunds on the surface runoff (R. Srinivasan 2014, pers. comm., 28 Oct.).

Manual calibration was used to elaborate a set of parameters sensitive to runoff and sediment yield for further investigation as well as trying to understand the hydrological and physical processes taking place in the study area. As already mentioned above, runoff events smaller than 0.15 mm were excluded from the calibration process to eliminate some of the events with the highest uncertainty (Zehetbauer 2014). SWAT CUP, particularly the SUFI-2 algorithm, was used for auto-calibration where 9 parameters were adjusted during the runoff calibration process and 3 were adjusted during the sediment calibration process.

The model was optimized by using the Nash-Sutcliffe efficiency (Nash & Sutcliffe 1970) as its common use provides extensive information on reported values (Moriasi et al. 2007). In addition two other parameters were used to evaluate the model performance, the Root-mean-squared error (RMSE) and the Kling-Gupta efficiency (Gupta et al. 2009).

The Nash-Sutcliffe efficiency (NSE) is calculated as follows:

$$NSE = 1 - \frac{\sum_{t=1}^{n}(Q_{s,t} - Q_{o,t})^2}{\sum_{t=1}^{n}(Q_{o,t} - Q_{o,mean})^2} \quad (3)$$

Where n is the number of time steps, $Q_{s,t}$ is the simulated value at time step t, $Q_{o,t}$ is the observed value at time step t, and $Q_{o,mean}$ is the mean of the observed values (Nash & Sutcliffe 1970). The NSE ranges between −infinite to 1.0, where NSE=1.0 is the optimum value. Values between 1.0 and 0 are generally considered as acceptable, whereas values ≤0.0 indicate, that the mean observed value is a better estimation than the simulated value (Moriasi et al. 2007).

Optimization with NSE tends to underestimate the peak runoff events (Gupta et al. 2009). However the peaks are the most interesting and reliable events (Zehetbauer 2014) for this study because they contribute the most to the development of the sub-watersheds in terms of changing the hydrological and sediment yield characteristics. Therefore a higher weight was given to higher runoff/sediment yield values during auto-calibration with SWAT-CUP in order to counteract this systematic underestimation and in order to make the model more reliable in estimating the runoff/sediment volume. SWAT-CUP provides an option of *Constant flow separation* in the Observed.txt file which allows the user to put weights on higher values (peak flows) or lower values (recessions). However this again lowers the NSE, as the optimum value regarding the peaks, when optimizing with NSE, would be lower. In other words, higher values for NSE would have been possible but by choosing to apply a higher weight to the runoff peaks the NSE was lowered. This has to be taken into consideration when interpreting the values for NSE.

The RMSE is calculated as follows:

$$RMSE = \sqrt{\frac{\sum_{t=1}^{n}(y_{s,t} - y_{o,t})^2}{\mathrm{n}}} \tag{4}$$

Where n is the number of time steps, $y_{s,t}$ is the simulated value at time step t and $y_{o,t}$ is the observed value at time step t. As the RMSE is scale dependant it has to be compared to the mean or standard deviation of the observed values in order to quantify the goodness of fit. A RMSE value of 0 would be the optimum value. Singh et al. (2004) state that RMSE values smaller than half the standard deviation of the observed data may be considered low.

The Kling-Gupta efficiency (KGE) is calculated as follows:

$$KGE = 1 - \sqrt{(r-1)^2 + (\alpha - 1)^2 + (\beta - 1)^2} \tag{5}$$

Where r is the linear regression coefficient between simulated and observed variable, α is the ratio between the standard deviation of the simulated and the standard deviation of the observed values, and β is the ratio between the mean simulated and the mean observed values. The KGE ranges from –infinite to 1.0 with the optimum value at KGE=1.0 (Gupta et al. 2009). Gupta et al. (2009) tried to show that there are systematic problems inherent with optimizations based on mean squared errors

(such as NSE) and therefore suggested an alternative criterion. Unfortunately there is almost no literature on the use of KGE, what makes is hard to qualify the values in terms of model evaluation.

Further the model performance was evaluated by comparing the mean volume of simulated runoff or sediment to the mean volume of observed runoff or sediment for a certain time period as well as the according standard deviation (Santhi et al. 2001).

In the SUFI-2 algorithm there are 2 measures to quantify the strength of a calibration/uncertainty analysis: The P-factor and the R-factor. The P-factor is the percentage of measured data bracketed by the 95 % prediction uncertainty (95PPU). The 95PPU is generated by parameter uncertainties which account for all sources of uncertainties such as uncertainty in driving variables (e.g. rainfall), conceptual model, parameters, and measured data. The 95PPU is calculated at the 2.5 % and 97.5 % levels of the cumulative distribution of an output variable obtained through Latin hypercube sampling (McKay et al., 2010), disallowing 5 % of the very bad simulations. The R-factor represents the average thickness of the 95PPU band divided by the standard deviation of the measured data. The P-factor has a range of 0 to 1, while the R-factor can reach from 0 to infinite. A simulation that exactly corresponds to measured data would be described by a P-factor of 1 and a R-factor of 0 (Abbaspour 2014).

3. Results and Discussion

3.1 Data Uncertainties

3.1.1 Uncertainty in Rainfall Data

As already mentioned above rainfall data was available from 1997 to 2013. Until the end of 2009 the rainfall data was monitored at a gauge respectively close to the study area, while starting with the year 2010 the rainfall data was monitored at a gauge situated within Aba-Kaloye sub-watershed (H.K. Addis 2014, pers. comm., 30 July). Zehetbauer (2014) reported that in the year 2012 for the rain gauge at Aba-Kaloye data was only available until 15.8.2012. The data in the time series for the model input was filled up with data of another rain gauge station within the Gumara-Maksegnit watershed about 4 km north of the rain gauge at Aba-Kaloye. This however led to high inconsistency regarding the runoff event at Ayaye sub-watershed on 16.8.2012, where 4.53 mm of runoff was observed while 0.2 mm of rainfall was monitored on the same day (Zehetbauer 2014). Based on that knowledge the runoff events on 16.8.2012 and 17.8.2012 were excluded from the calibration process.

For 2013 the data shows unusual high precipitation of 2087 mm. As it wasn't possible to verify this value and there were measurement errors reported at the weather station for 2013 (H.K. Addis 2014, pers. comm., 12 Oct.), it was excluded from the modeling period.

Zehetbauer (2014) reported an extremely high variable spatial distribution for the study area, which makes the importance of accurate rainfall monitoring evident, especially for the modeling of small area watersheds in that region.

3.1.2 Uncertainty in Calibration Data

The uncertainty in the observed runoff and sediment concentration data is most likely the predominant factor controlling model uncertainty (Addis et al. unpublished). Zehetbauer (2014) lists various reasons for data loss and erroneous data in the sub-catchments for the rainy season 2012. It can be assumed that the same uncertainties apply for the data of 2011.

Oscillations most likely due to insect activities were observed in the suspended sediment concentration measurements. Although insects' activity seems to influence

the signal more severe in between runoff events, an influence during runoff events is possible and cannot be excluded (Zehetbauer 2014).

Sedimentation and/or vegetation led to disturbance of the ultrasonic signal which was used to measure the height of the water table at the two gauging stations located at the two sub-watersheds' outlets. This led to high errors especially at small runoff events, while for bigger runoff events the uncertainty mainly affects the beginning and ending of an event (Zehetbauer 2014).

Initial wrong calibration of the ultrasonic measuring devices posed another problem. A transformation of the raw data had to be performed where several factors had to be estimated which led to uncertainties (Zehetbauer 2014).

Further the runoff/rainfall ratio shows high differences comparing the runoff data of 2011 to the one of 2012. An average runoff/rainfall ratio of 0.057 and 0.055 in 2011 and a runoff/rainfall ratio of 0.113 and 0.088 in 2012 was calculated for Aba-Kaloye sub-watershed and Ayaye sub-watershed respectively. The calculations are based on the sub-watersheds' area according to the SWAT model. Runoff events smaller 0.15 mm were excluded from the calculations. As there were no changes in soil conservation measures between 2011 and 2012 (H.K. Addis 2014, pers. comm., 29 Oct.), the high difference in the runoff/rainfall ratio could either be explained by processes in the study area which the author wasn't aware of, like for example conservation measures, tillage or cultivation practices, or by a systematic measurement error in one of the two years. The difference in the runoff/rainfall ratio can't be captured by the model unless the necessary information is provided in the form of model input data. As the data of 2012 is much more trustable as detailed studies have been carried out throughout the rainy season (Zehetbauer 2014), it was decided to use only the data of 2012 for calibration purposes.

3.1.3 Uncertainty of the DEM

The DEM was generated by using data collected with theodolites (H.K. Addis 2014, pers. comm., 2 Oct.), resulting in a resolution of about 5.02 m x 5.02 m. Nevertheless this is a rather high resolution interpolation processes to obtain the DEM for the whole study area cause high uncertainties regarding the slope steepness. Especially in a small study area of about 72 ha this parameter might be more sensitive regarding the runoff and soil loss than in a bigger watershed where it might average out (R. Srinivasan 2014, pers. comm., 28 Oct.).

Further the watershed boundaries in the SWAT model include an area of about 72 ha for both sub-watersheds (Aba-Kaloye 41.4 ha & Ayaye 30.5 ha), whereas Kluibenschädl (2014) suggests an area of 36 ha for Aba-Kaloye sub-watershed and Zehetbauer (2014) suggests an area of 24 ha for Ayaye sub-watershed. Hence there is a difference in the size of the study area of 12 ha, according to the watershed boundaries in the SWAT model based on the DEM.

3.2 Calibration Results

All calibration results are based on a model period from 2001-2012 with a warm up period of 5 years.

3.2.1 Crop Yield

Manual calibration was used for crop calibration. Guiding values for the average crop yield in the study area were available (Table 6). Fertilizer application (FRT_KG.mgt, FRT_SURFACE.mgt) (Table 9) for teff, wheat and barley and the adaption of the heat units to maturity (HEAT UNITS.mgt) for faba bean (HEAT UNITS.mgt = 1200) and chickpea (HEAT UNITS.mgt = 2000) was used to obtain acceptable crop yield modeling results.

Table 9: Overview of the applied fertilizer (Urea) for teff, wheat and barley at the planting date and one month after planting.

Fertilizer application - Urea			
	At planting	*+ 1 month*	
	FRT_KG	*FRT_KG*	*FRT_SURFACE*
Teff	100	80	0.2
Wheat	100	25	0.2
Barley	80	0	0.2
FRT_KG.mgt	Amount of fertilizer applied to HRU (kg/ha)		
FRT_SURFACE.mgt	Fraction of fertilizer applied to the first 10 mm of soil		

The calibration results are displayed in the following table (Table 10). It shows acceptable results mostly in the range of -200 to +100 kg/ha. The only exception is sorghum which’s crop yield is underestimated by approximately 300 kg/ha.

Table 10: Calibration results of the average crop yield.

	Teff *kg/ha*	**Sorghum** *kg/ha*	**Barley** *kg/ha*	**Wheat** *kg/ha*	**Chickpea** *kg/ha*	**Faba bean** *kg/ha*
Average crop yield	1700	1200	2400	2500	2600	3000
Simulated average crop yield	1531	896	2261	2588	2409	2951

3.2.2 Runoff Calibration

Manual calibration regarding the flow was used to elaborate a set of sensitive parameters for further investigation as well as trying to understand the hydrological and physical processes taking place in the study area. The two sub-watersheds are characterized by no baseflow, a low concentration time and short but intensive runoff events (Zehetbauer 2014). The main objective throughout the manual calibration process was to establish an interaction between the hydrological components which reflects the ongoing hydrological processes in the two sub-watersheds. Table 11 shows the parameters which were adjusted during the manual calibration process and the corresponding value.

Table 11: List of parameters adjusted during the manual calibration process with the corresponding value.

Parameter	**Value**
Ayaye & Aba-Kaloye sub-watershed, all land uses:	
CH_K2.rte	15
SHALLST.gw	500
GW_DELAY.gw	5
GWQMIN.gw	2500
ALPHA_BF.gw	0.1
GW_REVAP.gw	0.2
REVAPMN.gw	500
RCHRG_DP.gw	0.5
LAT_TTIME.hru	50
SLSOIL.hru	100
ESCO.hru	0.4
ICN.bsn	Plant ET Method
CNCOEF.bsn	0.5
Treated Ayaye sub-watershed, agricultural land uses:	
USLE_P.mgt	0.85
CN2.mgt	CN2*0.9

SWAT-CUP (SUFI-2 algorithm) was used for auto-calibration during which 9 parameters were adjusted. The following table (Table 12) shows a list of these

parameters with the corresponding initial value. For a short description of all the parameters mentioned in Table 11 and Table 12 see Table 13.

Table 12: List of the parameters adjusted during the auto-calibration process with the corresponding initial value.

Parameter	Initial value
Ayaye & Aba-Kaloye sub-watershed, all land uses:	
CH_K2.rte	15
GW_DELAY.gw	5
GWQMIN.gw	2500
ALPHA_BF.gw	0.1
REVAPMN.gw	500
ESCO.hru	0.4
CN2.mgt	CN2
Treated Ayaye sub-watershed, agricultural land uses:	
CN2.mgt	CN2*0.9
SLSUBBSN.hru	60
HRU_SLP.hru	3

Table 13: Short description of the parameters adjusted during manual and auto-calibration process (Arnold et al. 2012).

Parameter	Description
Ayaye & Aba-Kaloye sub-watershed, all land uses:	
CH_K2.rte	Effective hydraulic conductivity in main channel (mm/hr)
SHALLST.gw	Initial depth of water in shallow aquifer (mm H_2O)
GW_DELAY.gw	Ground water delay time (days)
GWQMIN.gw	Threshold depth of water in the shallow aquifer required for return flow to occur (mm H_2O)
ALPHA_BF.gw	Baseflow alpha factor (1/days)
GW_REVAP.gw	Ground water "revap" coefficient
REVAPMN.gw	Threshold depth of water in the shallow aquifer for "revap" or percolation to the deep aquifer to occur (mm H_2O)
RCHRG_DP.gw	Deep aquifer percolation fraction
LAT_TTIME.hru	Lateral flow travel time (days)
SLSOIL.hru	Slope length for lateral subsurface flow (m)
ESCO.hru	Soil evaporation compensation factor
ICN.bsn	Daily curve number calculation method
CNCOEF.bsn	Plant ET curve number coefficient
Treated Ayaye sub-watershed, agricultural land uses:	
USLE_P.mgt	USLE equation support practice factor
CN2.mgt	Initial SCS runoff curve number for moisture condition II
SLSUBBSN.hru	Average slope length (m)
HRU_SLP.hru	Average slope steepness (m/m)

The auto-calibration was performed for both sub-watersheds simultaneously as they are not hydrologically connected and therefore are not influencing each other. 500 simulations per iteration were run in SWAT-CUP. A total of 3 iterations were performed. The following table (Table 14) shows the parameters, their initial values for Iteration 3 with the corresponding range in SWAT-CUP and the fitted values as well as the final values for the last iteration for both sub-watersheds.

Table 14: Summary of the parameters and the corresponding initial value, range, fitted value and final value for Iteration 3 for both sub-watersheds.

Aba-Kaloye (untreated) - Iteration 3						
Parameter	*Initial value*	*Operator*	*Range*		*Fitted value*	*Final value*
CH_K2.rte	17.252001	v	16	20	17.204	17.204
GW_DELAY.gw	3.1096	a	-0.4	0.4	-0.2008	2.9088
GWQMN.gw	1372.800003	a	-200	200	86.800003	1459.600006
ALPHA_BF.gw	0.14845	v	0.1	0.15	0.14695	0.14695
REVAPMN.gw	894.400002	a	-100	100	21.000002	915.400004
ESCO.hru	0.3061	v	0.25	0.35	0.3271	0.3271
CN2.mgt	CN2*0.959777	r	-0.1	0.1	0.0006	CN2*0.9603528662
Ayaye (treated) - Iteration 3						
Parameter	*Initial value*	*Operator*	*Range*		*Fitted value*	*Final value*
CH_K2.rte	7.18	v	6	10	7.18	7.18
GW_DELAY.gw	0.9368	a	-0.4	0.4	-0.2792	0.6576
GWQMN.gw	3563.200012	a	-200	200	149.200012	3712.400024
ALPHA_BF.gw	0.15205	v	0.13	0.18	0.15205	0.15205
REVAPMN.gw	714	a	-100	100	93	807
ESCO.hru	0.3731	v	0.3	0.4	0.3731	0.3731
CN2.mgt	CN2*0.874095228	r	-0.1	0.1	-0.0006	CN2*0.8735707709
HRU_SLP.hru	HRU_SLP*1.4580058	r	-0.1	0.1	0.0246	HRU_SLP*1.493872743
SLSUBBSN.hru	SLSUBBSN*1.0596386	r	-0.1	0.1	0.0958	SLSUBBSN*1.161151978

There are three different methods to apply a range for a certain parameter which is specified by the operators *v*, *a* and *r*. The operator *v* means the existing value is to be replaced by the fitted value, the operator *a* means the fitted value is added to the existing value and the operator *r* means the existing value is multiplied by (1+ a fitted value) (Abbaspour 2014).

The following diagrams (Figure 20 and Figure 21) show the results of the auto-calibration with SWAT-CUP. The events of 2012 listed in Table 7 are represented on the x-axis and the runoff in mm is indicated on the y-axis. The plot shows the

observed values (blue graph), the best simulation (red graph) and the upper/lower limit of the 95 % probability uncertainty (95PPU). The 95PPU, as already mentioned above, is calculated at the 2.5 % and 97.5 % levels of the cumulative distribution of an output variable obtained through Latin hypercube sampling (McKay et al. 2010), disallowing 5 % of the very bad simulations (Abbaspour 2014).

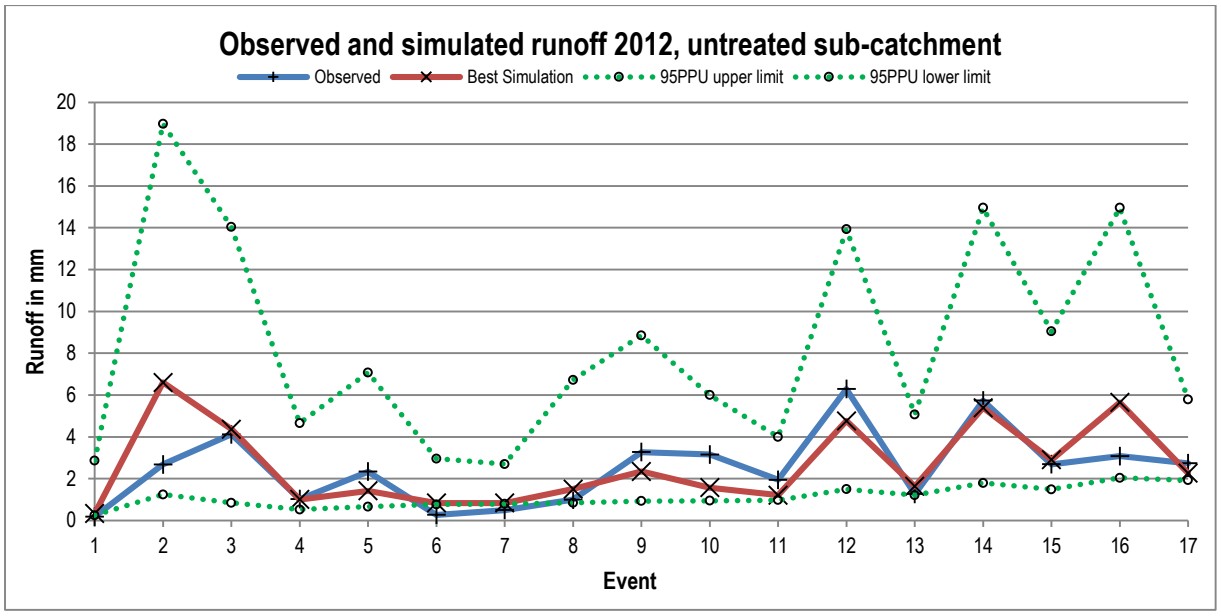

Figure 20: Runoff plot of the observed values, the best simulation and the 95% probability uncertainty band according to auto-calibration with SWAT-CUP for the untreated Aba-Kaloye sub-catchment.

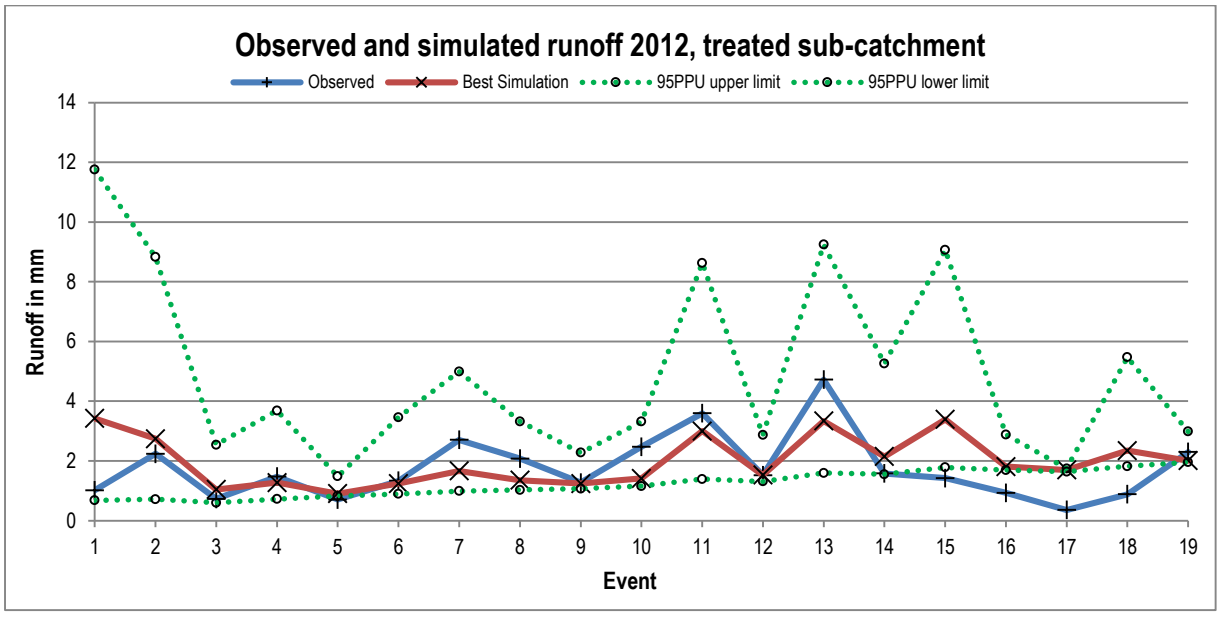

Figure 21: Runoff plot of the observed values, the best simulation and the 95% probability uncertainty band according to auto-calibration with SWAT-CUP for the treated Ayaye sub-catchment.

For both sub-watersheds it is evident that the higher runoff events involve a higher model prediction uncertainty, as the thickness of the 95PPU is much bigger for the peak runoffs than for low flow events. Further it is notable that in both sub-

watersheds some observed events are not bracketed by the 95PPU band. This means that the model isn't able to capture these events, which involve solely low flow events, at all. In the untreated Aba-Kaloye sub-catchment event number 2 and 16 are clearly overestimated by approximately 3.5 mm, whereas events number 9 to 12 are underestimated by approximately 1 mm. In the treated Ayaye sub-catchment the 1st event and events number 14-18 are overestimated, while event number 1 and 15 are overestimated by approximately 1 to 2 mm. On the other hand events number 7, 8, 10, 11 and 13 are underestimated by approximately 0.5 to 1 mm.

The following figures (Figure 22 and Figure 23) show a scatter plot of the observed versus the simulated runoff data 2012 for both sub-watersheds. It shows how well the regression line fits the 1:1 line and if the model in average is under or overestimating. Both plots show a narrow fit of the regression line to the 1:1 line. The untreated Aba-Kaloye sub-catchment however performs better since the majority of the runoff events are closer to the 1:1 line compared to the treated Ayaye sub-catchment.

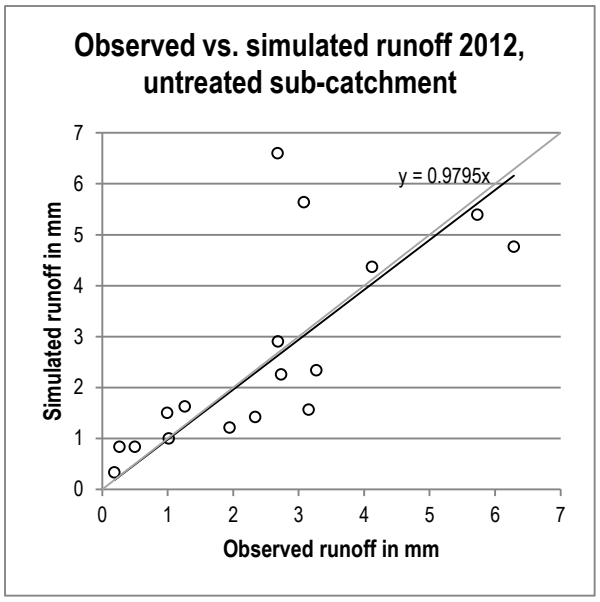

Figure 22: Scatter plot of the observed vs. the simulated runoff data 2012 for the untreated Aba-Kaloye sub-catchment.

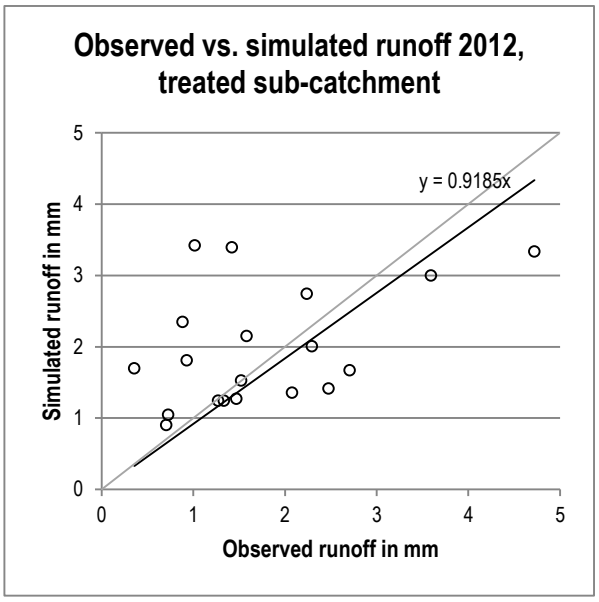

Figure 23: Scatter plot of the observed vs. the simulated runoff data 2012 for the treated Ayaye sub-catchment.

As mentioned above, several parameters were used to assess the goodness of fit. The following table (Table 15) shows an overview of the different parameters with the according value for both sub-watersheds.

Table 15: Overview of parameters for evaluating the goodness of fit for both sub-watersheds.

Evaluation of the model fit - Aba-Kaloye (untreated)								
NSE	*RMSE*	*KGE*	*Mean Vs*	*Mean Vo*	*St.Dev. Vs*	*St.Dev. Vo*	*p-factor*	*r-factor*
0.39	1.34 mm	0.71	2.62 mm	2.49 mm	0.83 mm	1.08 mm	0.82	0.59
Evaluation of the model fit - Ayaye (treated)								
NSE	*RMSE*	*KGE*	*Mean Vs*	*Mean Vo*	*St.Dev. Vs*	*St.Dev. Vo*	*p-factor*	*r-factor*
0.04	1.03 mm	0.38	1.98 mm	1.75 mm	1.96 mm	1.76 mm	0.79	0.25

NSE…… Nash-Sutcliffe efficiency (Nash & Sutcliffe 1970)
RMSE……. Root-mean-squared error
KGE…… Kling-Gupta efficiency (Gupta et al. 2009)
Mean Vs…… Mean simulated flow volume
Mean Vo…… Mean observed flow volume
St.Dev. Vs…. Standard deviation of simulated flow volume
St.Dev. Vo…. Standard deviation of observed flow volume
p-factor…….. p-factor according to SUFI-2 algorithm (Abbaspour 2014)
r-factor……. r-factor according to SUFI-2 algorithm (Abbaspour 2014)

According to Moriasi et al. (2007) a NSE value between 0.0 and 1.0 are viewed as acceptable levels of performance, as all values >0.0 mean that the model is able to capture paterns of the observed data. A positive NSE was achieved for both sub-watersheds, 0.39 for the untreated Aba-Kaloye sub-watershed and 0.04 for the treated Ayaye sub-watershed. As already mentioned in chapter 2.6, it has to be taken into consideration, that the NSE was lowered by applying a higher weight on the runoff peaks during auto-calibration in order to make the model more reliable in estimating the peaks and therefore the runoff volume. By doing so the NSE reduced itself from 0.48 to 0.39 and from 0.14 to 0.04 for the untreated and treated sub-watershed respectively. It is evident that the model performs significantly better for the untreated sub-watershed than for the treated sub-watershed, according to the NSE values.

RMSE values can be considered high for both sub-watersheds since the values are not less than half of the standard deviation of the according observed data (Untreated Aba-Kaloye sub-watershed: RMSE=1.34 mm, 0.5*St.Dev.Vo=0.54 mm; treated Ayaye sub-watershed: RMSE=1.03 mm, 0.5*St.Dev.Vo=0.88 mm) (Singh et al. 2004). Regardless of their unsatisfying magnitude, according to the RMSE values the model seems to perform better for the treated Ayaye sub-watershed.

A KGE value of 0.71 and 0.38 was achieved for the untreated and for the treated sub-catchment respectively. Since it's hard to find any study using the KGE criterion for model evaluation it's hard to qualify the values. However it is interesting that the KGE stayed the same for Aba-Kaloye sub-watershed (0.71) and improved for Ayaye sub-watershed (from 0.28 to 0.38) after applying a higher weight to the higher runoff values. As for the KGE the optimal value is 1.0 (Gupta et al. 2009) it can be assumed that the obtained values show a satisfying to acceptable result.

Means and standard deviations of the observed and simulated flow Volumes are within a difference of approximately 6 and 24 % and 14 and 12 % for the untreated Aba-Kaloye sub-watershed and the treated Ayaye sub-watershed respectively.

In the SUFI-2 algorithm used in SWAT-CUP the P-factor and the R-factor are good indicators for quantifying the strength of the calibration and uncertainty of the model, as already described in chapter 2.6. The P-factor in both sub-watersheds is satisfying with approximately 0.8. Considering the R-factor ranges from 0 to infinite with its optimum value at 0, the obtained values for the untreated (0.59) and treated (0.25) sub-watersheds can be considered as satisfying. However Figure 20 and Figure 21 show that for some events the thickness of the 95PPU band still shows high values and therefore a high uncertainty.

3.2.2.1 Runoff Calibration Summary

Nevertheless the model shows satisfying performance, for the treated Aba-Kaloye sub-watershed, and acceptable performance, for the untreated Ayaye sub-watershed, regarding the runoff. Since sub-daily processes govern the watershed hydrology, it can be assumed that the model could be performing better with data on a sub-daily scale. A suitable algorithm was developed by Jeong et al. (2010). However, it remains open to question to which degree this would improve the model performance and if this would justify the increased effort for data collection.

3.2.3 Sediment Calibration

During manual and auto-calibration regarding the sediment 3 parameters were adjusted: The P-factor (USLE_P.mgt), the K-factor (USLE_K.sol) and the C-factor (USLE_C.plant) of the MUSLE equation (Williams 1975). Table 16 shows a short description of these 3 parameters.

Table 16: Short description of the parameters adjusted during manual and auto-calibration process (Arnold et al. 2012).

Parameter	Description
Ayaye & Aba-Kaloye sub-watershed:	
USLE_K.sol	USLE equation soil erodibility factor
USLE_C.plant	USLE C factor for water erosion applicable to the land cover/plant
Treated Ayaye sub-watershed:	
USLE_P.mgt	USLE equation support practice factor

As already mentioned above the P-factor of course was only adjusted for the treated Ayaye sub-watershed and it was set to 0.85. The K-factor was recalculated, as the K-factors in the available soil data were not plausible. Schwertmann et al. (1987) developed an equation for estimating the K-factor for European soils. This equation yielded more appropriate results for the soils in the study area than the equation of Wischmeier & Smith (1978), which was developed for American soils, and was therefore used for recalculating the K-factor.

$$K = 2.77 * 10^{-6} * M^{1.14} * (12 - OS) + 0.043 * (A - 2) + 0.0033 * (4 - D) \quad (6)$$

Where K is the K-factor, M is the particle-size parameter, OS is the % organic matter, A is the soil structure code used in soil classification and D is the permeability class of the profile. M is calculated as follows (Schwertmann et al. 1987):

$$M = (m_{silt} + m_{vfs}) * (100 - m_{clay}) \quad (7)$$

Where m_{silt} is the % silt content, m_{vfs} is the % very fine sand content and m_{clay} is the % clay content. OS can be estimated as follows (Schwertmann et al. 1987):

$$OS = 1.72 * OrgC \quad (8)$$

Where $OrgC$ is the % organic carbon content. Table 17 shows the soil structure codes with the according mean aggregate size and size classes, whereas Table 18 shows the permeability classes with the permeability code and the according hydraulic conductivity of the profile (Schwertmann et al. 1987, Wischmeier & Smith 1978).

Table 17: Soil structure codes used in Formula (6) with the according size classes and mean aggregate sizes.

Size class	Soil structure code	Mean aggregate size (mm)
very fine granular	1	<1
fine granular	2	1-2
medium or coarse granular	3	2-10
blocky, platty or massive	4	>10

Table 18: Permeability codes used in Formula (6) with the according permeability classes and the hydraulic conductibity.

Permeability class	Permeability code	Hydraulic conductivity (cm/d)
very slow	1	<1
slow	2	1-10
slow to moderate	3	10-40
moderate	4	40-100
moderate to rapid	5	100-300
rapid	6	>300

The C-factors were reassessed, as the default values in SWAT are not suitable for the conditions in the study area. Kaltenrieder (2007) developed an adapted USLE for the Ethiopian-Eritrean Highlands and therefore suggested adapted C-factors for this region. The following table (Table 19) shows the chosen value for the C-factor for each crop growing in the study area.

Table 19: Reassessed C-Factors for each crop growing in the study area. Values are based on the findings of Kaltenrieder (2007).

Land use	Land use in SWAT	C-Factor
Eragrostis Teff	Eragrostis Teff	0.50
Sorghum	Grain sorghum	0.20
Barley	Spring barley	0.30
Wheat	Spring wheat	0.40
Chickpea	Lentils	0.35
Faba bean	Lentils	0.35

As for the runoff calibration the auto-calibration for sediment was performed using SWAT-CUP with 500 simulations running per iteration. One iteration was performed. The auto-calibration was performed separately for the USLE_P.mgt paramter whereas it was performed together for the USLE_C.plant and the USLE_K.sol parameters. The following table (Table 20) shows the parameters, their initial values

for Iteration 1 with the corresponding range in SWAT-CUP and the fitted values as well as the final values for the last iteration for both sub-watersheds.

Table 20: Summary of the parameters and the corresponding initial value, range, fitted value and final value for Iteration 1 for both sub-watersheds.

Aba-Kaloye (untreated) - Iteration 1						
Parameter	*Initial value*	*Operator*	*Range*		*Fitted value*	*Final value*
USLE_C.plant	see Table 19	r	-0.1	0.1	0.0794	USLE_C*1.0794
USLE_K.sol	USLE_K*1.1	r	-0.2	0.2	-0.0772	USLE_K*1.01508
Ayaye (treated) - Iteration 1						
Parameter	*Initial value*	*Operator*	*Range*		*Fitted value*	*Final value*
USLE_P.mgt	0.85	r	-0.05	0.05	0.0473	0.890205
USLE_C.plant	see Table 19	r	-0.1	0.1	0.0794	USLE_C*1.0794
USLE_K.sol	USLE_K*1.1	r	-0.2	0.2	-0.0772	USLE_K*1.01508

There are three different methods to apply a range for a certain parameter where the operator *r* means the existing value is multiplied by (1+ a fitted value) (Abbaspour 2014).

The following diagrams (Figure 24 and Figure 25) show the results of the auto-calibration with SWAT-CUP. The events listed in Table 8 are represented on the x-axis and the sediment yield in t/ha is indicated on the y-axis. The plot shows the observed values (blue graph), the best simulation (red graph) and the upper/lower limit of the 95 % probability uncertainty (95PPU). The 95PPU, as already mentioned above, is calculated at the 2.5 % and 97.5 % levels of the cumulative distribution of an output variable obtained through Latin hypercube sampling (McKay et al. 2010), disallowing 5 % of the very bad simulations (Abbaspour 2014).

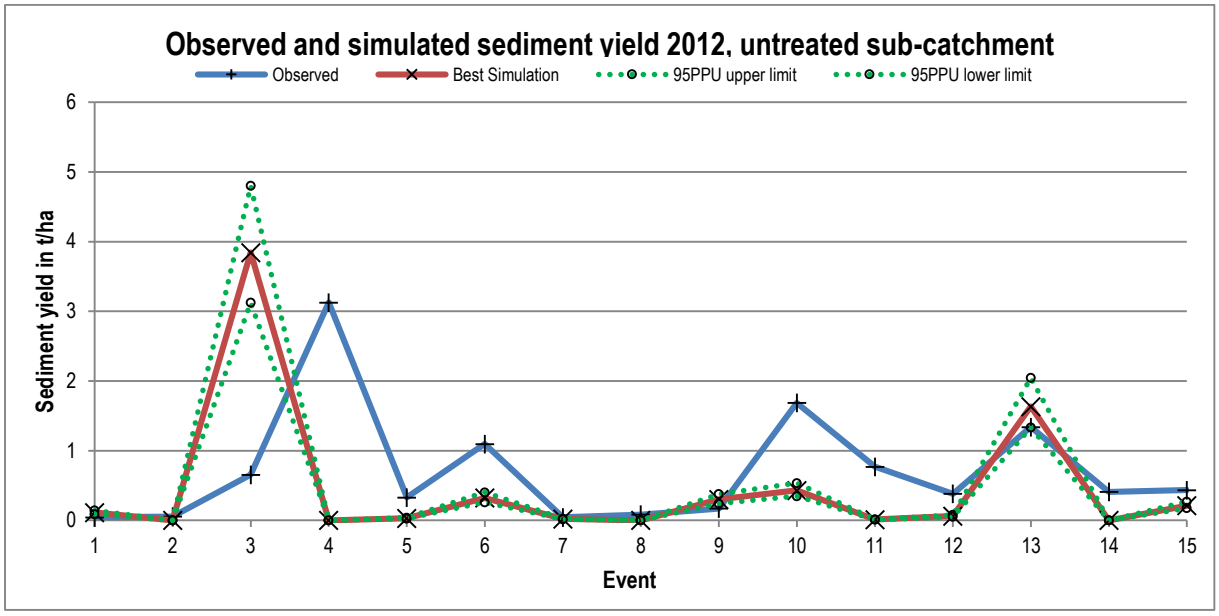

Figure 24: Sediment yield plot of the observed values, the best simulation and the 95% probability uncertainty band according to auto-calibration with SWAT-CUP for the untreated Aba-Kaloye sub-catchment.

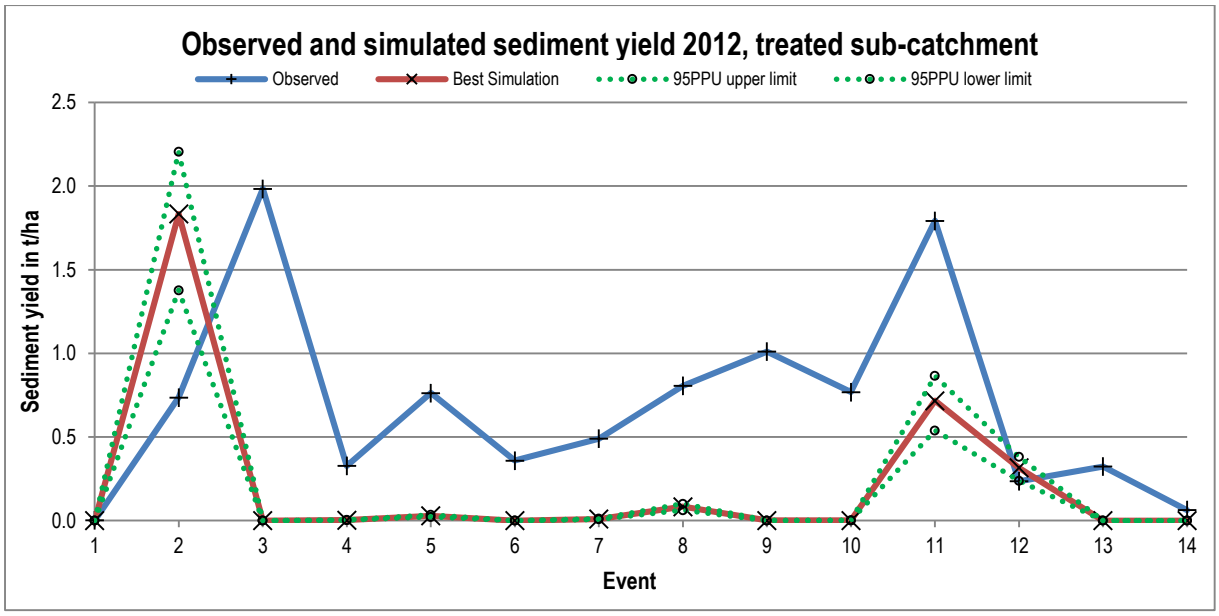

Figure 25: Sediment yield plot of the observed values, the best simulation and the 95% probability uncertainty band according to auto-calibration with SWAT-CUP for the treated Ayaye sub-catchment.

It is clearly evident that for both sub-watersheds the model is significantly underestimating nearly all of the events in the calibration period. Some events are even simulated with a sediment yield of 0. Only a very small percentage close to 0 is bracketed by the 95PPU band. In both sub-watersheds there is a clear shift in the beginning of the calibration period (event 3/4 and event 2/3 respectively). This problem of different ratios of rainfall to sediment yield for some events was already addressed above in chapter 2.5.2.2 and it is obvious that the model is not able to take that into account. In general the untreated sub-catchment performs better than

the treated sub-catchment since the model is able to capture the pattern better. For the treated sub-watershed the majority of the events (9 out of 14) are simulated very close to 0 and therefore nearly no pattern is visible.

The following figures (Figure 26 and Figure 27) show a scatter plot of the observed versus the simulated runoff data 2012 for both sub-watersheds. It shows how well the regression line fits the 1:1 line and if the model in average is under or overestimating. Both plots show an unsatisfying fit of the regression line to the 1:1 line. The untreated Aba-Kaloye sub-catchment however performs a little bit better. The overestimating outlier in both plots is due to the shift in the beginning of the calibration period.

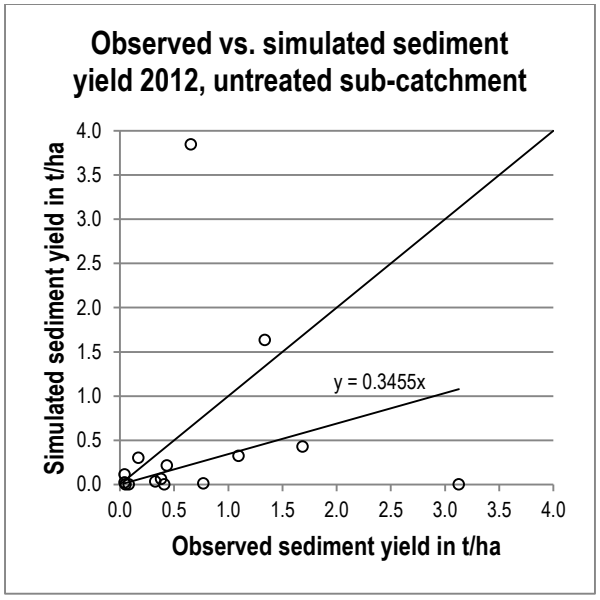

Figure 26: Scatter plot of the observed vs. the simulated sediment yield data 2012 for the untreated Aba-Kaloye sub-catchment.

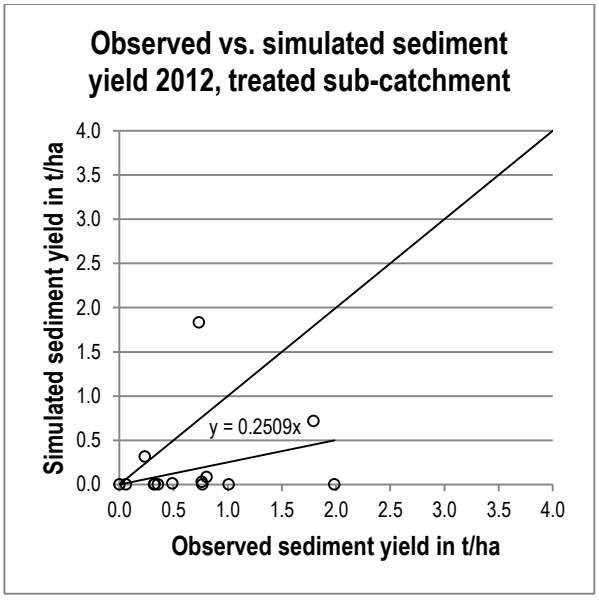

Figure 27: Scatter plot of the observed vs. the simulated sediment yield data 2012 for the treated Ayaye sub-catchment.

As mentioned above, several parameters were used to assess the goodness of fit. The following table (Table 21) shows an overview of the different parameters with the according value for both sub-watersheds.

Table 21: Overview of parameters for evaluating the goodness of fit for both sub-watersheds.

Evaluation of the model fit - Aba-Kaloye (untreated)								
NSE	*RMSE*	*KGE*	*Mean Vs*	*Mean Vo*	*St.Dev. Vs*	*St.Dev. Vo*	*p-factor*	*r-factor*
-1.38	1.24 t/ha	0.00	0.47 t/ha	0.71 t/ha	1.02 t/ha	0.84 t/ha	0.07	0.25
Evaluation of the model fit - Ayaye (treated)								
NSE	*RMSE*	*KGE*	*Mean Vs*	*Mean Vo*	*St.Dev. Vs*	*St.Dev. Vo*	*p-factor*	*r-factor*
-1.12	0.83 t/ha	-0.07	0.21 t/ha	0.69 t/ha	0.51 t/ha	0.59 t/ha	0.07	0.17

NSE	Nash-Sutcliffe efficiency (Nash & Sutcliffe 1970)
RMSE	Root-mean-squared error

KGE	Kling-Gupta efficiency (Gupta et al. 2009)
Mean Vs	Mean simulated sediment yield volume
Mean Vo	Mean observed sediment yield volume
St.Dev. Vs	Standard deviation of simulated sediment yield volume
St.Dev. Vo	Standard deviation of observed sediment yield volume
p-factor	p-factor according to SUFI-2 algorithm (Abbaspour 2014)
r-factor	r-factor according to SUFI-2 algorithm (Abbaspour 2014)

A NSE value ≤0.0 indicates that the mean observed value is a better estimator than the simulated value (Moriasi et al. 2007). Unfortunately this is the case regarding the sediment calibration. The NSE is -1.38 and -1.12 for the untreated Aba-Kaloye sub-watershed and for the treated Ayaye sub-watershed respectively. Again, as mentioned in chapter 2.6, it has to be considered, that the NSE was lowered by applying a higher weight on the peak events during auto-calibration in order to try to make the model more reliable in estimating the peaks and therefore the sediment yield volume. This changed the NSE from -0.97 to -1.38 and from -1.05 to -1.12 for the untreated and for the treated sub-catchment respectively. This shows that the value was already negative before applying a higher weight to the peak events. The treated sub-watershed performs slightly better than the untreated one. Nevertheless, according to the NSE, the model performance for both sub-catchments is unacceptable.

RMSE values can be considered high for both sub-watersheds since the values are not less than half of the standard deviation of the according observed data (Untreated Aba-Kaloye sub-watershed: RMSE=1.24 t/ha, 0.5*St.Dev.Vo=0.42 t/ha; untreated Ayaye sub-watershed: RMSE=0.83 t/ha, 0.5*St.Dev.Vo=0.30 t/ha) (Singh et al. 2004). The values of the RMSE even exceed the values of the standard deviations, what shows that the model performs poorly for both sub-watersheds.

As already mentioned above, it's hard to find any study using the KGE criterion for model evaluation what makes it hard to qualify the values. However as for the KGE the optimal value is 1.0 (Gupta et al. 2009) it can be assumed that the obtained values (Untreated sub-watershed: 0.00; treated sub-watershed: -0.07) indicate a unsatisfying to unacceptable model performance. Still it is notable that the KGE improved for both sub-watersheds after applying a higher weight to the higher runoff

values. It changed from -0.03 to 0.00 and from -0.16 to -0.07 in the untreated and in the treated sub-catchment respectively.

Means and standard deviations of the observed and simulated sediment yield Volumes are within a difference of approximately 34 and 22 % and 69 and 14 % for the untreated Aba-Kaloye sub-watershed and the treated Ayaye sub-watershed respectively. This shows a high difference, especially regarding the mean observed and simulated sediment yield volumes.

As already described in chapter 2.6, in the SUFI-2 algorithm used in SWAT-CUP the P-factor and the R-factor are good indicators for quantifying the strength of the calibration and uncertainty of the model. The P-factor in both sub-watersheds is unsatisfying with approximately 0.07. The R-factor has its optimum value at 0 and the achieved values of 0.25 for the untreated and 0.17 for the treated sub-catchment are rather low. Nevertheless for proper model evaluation the P-factor and R-factor have to be evaluated together. Therefore the model shows an unsatisfying performance, since only 7 % of the observed data are bracketed by the 95PPU band, regardless of the relatively low R-factor values.

As the model performance regarding the sediment on a daily basis is unacceptable, it was decided to investigate the model results on an annual basis. The following table (Table 22) shows the annual budgets for the years 2006 to 2012 with the according rainfall and the mean annual budget. The model period was 2001 to 2012 and the warm up period was 5 years. The values seem plausible for nearly all of the years. In 2011, however, the sediment yield is exceptionally high for both sub-watersheds. Further this is the only year in the simulation during which the sediment yield is higher in the treated than in the untreated sub-watershed. Addis et al. (2013) reported a soil loss rate of 20-25 t/ha for a superordinate sub-basin in which the study area is located. Since the study area is known to have severe soil loss problems and higher sediment yield rates can be expected, the obtained values for the mean annual sediment yield of 37.8 t/ha and 32.4 t/ha for the untreated and for the treated sub-watersheds respectively can be considered as plausible and therefore as satisfying.

Table 22: Annual sediment yield budgets for the years 2006 to 2012 with the according rainfall and the mean annual budget.

Year	Rainfall	Aba-Kaloye, untreated		Ayaye, treated	
	mm	*t*	*t/ha*	*t*	*t/ha*
2006	1482	1278	30.9	584	19.1
2007	1480	1228	29.7	405	13.3
2008	1206	1357	32.8	747	24.5
2009	1041	1431	34.6	838	27.5
2010	1119	1667	40.3	940	30.8
2011	1397	3223	77.9	3211	105.3
2012	942	761	18.4	199	6.5
		Mean:	37.8	*Mean:*	32.4

3.2.3.1 Sediment Calibration Summary

The results for sediment calibration on a daily basis show, that there are problems incorporated in the model simulation. The major problem remains the sub-daily characteristics of erosion and sediment transport processes in the study area, which are not reflected by the underlying daily based data (also see chapter 2.5.2.2). Jeong et al. (2011) developed an algorithm for sub-daily erosion and sediment transport processes to improve the model capacities, especially for small watersheds with a low concentration time where sub-daily processes govern the watershed hydrology. Therefore it would be necessary to collect the data on a sub-daily scale, to be able to implement this algorithm in the model. Again, it remains open to question if the model would be improved to such a degree by which the increased effort for data collection is justified. Another problem during the calibration process was the absolute insensitivity of the parameters governing the channel erosion process (e.g.: CH_N2.rte, CH_COV1.rte, CH_COV2.rte, SPCON.rte) as well as the channel geometry, which did not influence the sediment output at all. Hence it remains the question how high SWAT's capability is to model the soil loss in small watersheds (<45 ha) with high rainfall intensities, low concentration times and high soil erosion rates in a satisfying way.

4. Summary and Conclusion

The objective of this master thesis was the establishment of a calibrated SWAT model for the two sub-watersheds in Ethiopian Highlands, Aba-Kaloye and Ayaye. Further the effects of SWC measures in the treated Ayaye sub-watershed in comparison to the untreated Aba-Kaloye sub-watershed should be evaluated. The findings should then be used for up-scaling of SWC impacts, to gain a deeper insight into SWC interactions at sub-watershed level related to hydrological and land degradation issues.

Calibration of the SWAT model for runoff and sediment data was performed with SWAT-CUP for two sub-watersheds. The model performance was evaluated with different parameters and criterions. A calibrated SWAT model was established regarding the flow. The model shows an unacceptable soil loss fit, and can therefore not be considered as calibrated regarding the sediment. Hence the model could not be used to evaluate the effects of the SWC measures in the treated Ayaye sub-watershed. Further it could not be used for up-scaling of SWC impacts.

A key problem throughout this whole study was the data uncertainty and data scarcity regarding the runoff as well as the sediment data. Therefore only a small number of events within one rainy season were available for calibration purposes. As already mentioned above, it can be assumed, that sub-daily rainfall and sediment data would be more suitable for modeling the study area and would lead to a better model performance. As the model still isn’t in its final stage the findings of following field experiments and more observation years for calibration, and especially validation, have to be included.

5. References

Abbaspour, K.C., 2014. SWAT-CUP 2012: SWAT Calibration and Uncertainty Programs - A User Manual.

Addis, H.K., Strohmeier, S., Srinivasan, S., Ziadat, F., Klik, A., 2013. Using SWAT model to evaluate the impact of community-based soil and water conservation interventions for an Ethiopian watershed. In SWAT 2013 Conference Proceedings.

Addis, H.K., Strohmeier, S., Srinivasan, S., Ziadat, F., Klik, A., unpublished. Using the SWAT Model to Evaluate the Impact of Soil and Water Conservation Interventions on Mountainous Watershed in North Gonder, Ethiopia.

Arnold, J.G., Kiniry, J.R., Srinivasan, R., Williams, J.R., Haney, E.B., Neitsch, S.L., 2012. Soil & Water Assessment Tool Input/Output Documentation, Version 2012.

Arnold, J.G., Williams, J.R., Maidment, D.R., 1995. Continuous-Time Water and Sediment-Routing Model for Large Basins. Journal of Hydraulic Engineering, 121(2), pp.171–183.

Blanco, H. & Lal, R., 2008. Principles of Soil Conservation and Management, Columbus, Ohio: Springer.

Bosshart, U., 1997. Catchment Discharge and Suspended Sediment Transport as Indicators of Physical Soil and Water Conservation in the Mayketin Catchment, Afdeyu Research Unit: A Case Study in the Northern Highlands of Eritrea (Volume 39 of Soil conservation research project: research report). University of Bern, Bern.

Brenner, C., 2013. Monitoring and Simulation of Soil Erosion in the Ethiopian Highlands on a Plot Scale. University of Natural Resources and Life Sciences, BOKU Vienna.

Dejene, A., 2003. Natural Resources Management to Enhance The Case for Community-Based, Rome: FAO.

FAO, 1986. Ethiopian Highland Reclamation Study, Final Report, Rome.

GARC, 2010. Socio-economic survey of Gumara-maksegnit watershed. Gondar, Ethiopia: ICARDA, ARARI, EIAR, BOKU, SASKAWA.

Gupta, H.V., Kling, H., Yilmaz, K.K., Martinez, G.F., 2009. Decomposition of the mean squared error and NSE performance criteria: Implications for improving hydrological modelling. Journal of Hydrology, 377(1-2), pp.80–91.

Hurni, H., 1988. PART 2 : Degradation and Conservation of the Resources in the Ethiopian Highlands. Mountain Research and Development, 8, pp.123–130.

ICARDA 2014, Community based rainfed watershed management. Available from: http://rainfedsystems.icarda.org/. [7 May 2015].

Jeong, J., Kannan, N., Arnold, J., Glick, R., Gosselink, L., Srinivasan, R., 2010. Development and Integration of Sub-hourly Rainfall-Runoff Modeling Capability Within a Watershed Model. Water Resources Management, 24(15), pp.4505–4527.

Jeong, J., Kannan, N., Arnold, J., Glick, R., Gosselink, L., Srinivasan, R., Harmel, R.D., 2011. Development of Sub-Daily Erosion and Sediemtn Transport Algorithms for SWAT. Transactions of the ASABE, 54(5), pp.1685–1691.

Kaltenrieder, J., 2007. Adaptation and Validation of the Universal Soil Loss Equation (USLE) for the Ethiopian-Eritrean Highlands. Faculty of Science.

Kluibenschädl, F., 2014. Assessment of gully erosion investigation methods by linking a photogrametic approach and field measurements. University of Natural Resources and Life Sciences, BOKU Vienna.

Knisel, W.G., 1980. CREAMS, A Field Scale Model for Chemicals / Runoff , and Erosion From Agricultural Management Systems, USDA Conservation Research Report No. 26.

Lawler, D.M., Thorne C.R., Hooke, J.M. 1997. Bank erosion and instability, in Thorne, C.R., Hey, R.D., Newson, M.D. (Eds), Applied Fluvial Geomorphology for River Engineering and Management, Chichester, 137-172.

Leonard, R.A., Knisel, W.G., Still, D.A., 1987. GLEAMS, Groundwater Loading Effects of Agricultural Management Systems. Transactions of ASAE, 30(5), pp.1403–1418.

McKay, M.D., Beckman, R.J., Conover, W.J., 2010. Methods Comparison of Three Variables in the of Values Input a From Computer Code Output Selecting of Analysis for. Technometrics, 42(1), pp.55–61.

Mengistu, A., 2006. Country Pasture / Forage Resource Profiles - Ethiopia, Addis Abeba.

Moriasi, D.N., Arnold, J.G., Van Liew, M.W., Bingner, R.L., Harmel, R.D., Veith, T.L., 2007. Model Evaluation Guidelines for Systematic Quantification of Accuracy in Watershed Simulations. Transactions of the ASABE, 50(3), pp.885–900.

Nash, J.E. & Sutcliffe, J.V, 1970. River Flow Forecasting Through Conceptual Models Part 1 - A Discussion of Principles. Journal of Hydrology, 10, pp.282–290.

Neitsch, S.L., Arnold, J.G., Kiniry, J.R., Williams, J.R., 2011. Soil & Water Assessment Tool Theoretical Documentation, Version 2009.

Nyssen, J., Poesen, J., Moeyersons, J., Deckers, J., Haile, M., Lang, A., 2004. Human impact on the environment in the Ethiopian and Eritrean highlands—a state of the art. Earth-Science Reviews, 64(3-4), pp.273–320.

Nyssen, J., Poesen, J., Haile, M., Moeyersons, J., Deckers, J., 2000. Tillage erosion on slopes with soil conservation structures in the Ethiopian highlands. Soil and Tillage Research, 57(3), pp.115–127.

Oldeman, L.R., 1992. Global Extent of Soil Degradation. ISRIC Bi-Annual Report 1991-1992, pp.19–36.

Santhi, C., Arnold, J.G., Williams, J.R., Dugas, W.A., Srinivasan, R., Hauck, L.M., 2001. Validation of the SWAT Model on a Large River Basin with Point and Nonpoint Sources. Journal of the American Water Resources Association, 37(5), pp.1169–1188.

Saxton, K.E. & Rawls, W.J., 2006. Soil Water Characteristic Estimates by Texture and Organic Matter for Hydrologic Solutions. Soil Science Society of America Journal, 70, pp.1569–1578.

Scherr, S.J. & Yadav, S., 1996. Land Degredation in the Developing World Implications for Food, Agriculture, and the Environment to 2020, Washington, D.C.: IFPRI.

Schwertmann, U., Vogl, W., Kainz, M. 1987. Bodenerosion durch Wasser. Vorhersage des Abtrags und Bewertung von Gegenmaßnahmen. Stuttgart.

Sharpley, N. & Williams, J.R., 1990. EPIC: The erosion-productivity impact calculator, 1. model documentation. U.S. Department of Agriculture, Agricultural Research Service, Technical Bulletin 1768.

Singh, J., Knapp, H.V., Demissie, M., 2004. Hydrologic modeling of the Iroquois River watershed using HSPF and SWAT. ISWS CR 2004-08. Champaign, Ill.: Illinois State Water Survey.

Sonneveld, B.G.J.S. & Keyzer, M.A., 2003. Land under pressure: Soil conservation concerns and opportunities for Ethiopia. Land Degradation & Development, 14, pp.5–23.

Taddese, G., 2001. Land Degradation: A Challenge to Ethiopia. Environmental Management, 27(6), pp.815–824.

Tebebu, T.Y., Abiy, A.Z., Zegeye, A.D., Dahlke, H.E., Easton, Z.M., Tilahun, S.A., Collick, A.S., Kidnau, S., Moges, S., Dadgari, F., Steenhuis, T.S., 2010. Surface and subsurface flow effect on permanent gully formation and upland erosion near Lake Tana in the northern highlands of Ethiopia. Hydrology and Earth System Sciences, 14, pp.2207–2217.

Williams, J.R., 1969. Flood Routing with Variable Travel Time or Variable Storage Coefficients. Transactions of the ASAE, 12(1), pp.100–103.

Williams, J.R., 1975. Sediment-yield predictoin with universal equation using runoff energy factor. In Present and Prospective Technology for Predictiong Sediment Yields and Sources. Oxford, MS, November 28- 30, 1972: USDA Sedimentation Laboratory, pp. 244–252.

Williams, J.R., Jones, C.A., Dyke, P.T., 1984. A Modeling Approach to Determining the Relationship Between Erosion and Soil Productivity. Transactions of ASAE, pp.129–144.

Williams, J.R., Nicks, A.D., Arnold, J.G., 1985. Simulator for Water Resources in Rural Basins. Journal of Hydraulic Engineering, 111(6), pp.970–986.

Wischmeier, W.H. & Smith, D.D., 1978. Predicting Rainfall Erosion Losses - A Guide to Conservation Planning. Agriculture Handbook, 537.

Zehetbauer, I., 2014. Runoff and Sediment Monitoring in an Agricultural Watershed in the Ethiopian Highlands. University of Natural Resources and Life Sciences, BOKU Vienna.

6. List of Figures

7. Table Directory

8. Appendix

8.1 Crop Management schemes in SWAT

Eragrostis Teff - Sorghum - Chickpea			141021TEFF	
Year	*Month*	*Day*	*Management operation*	*Specification*
1	1	15	Harvest and kill operation	
1	4	28	Tillage operation	Generegic Conservation Tillage
1	5	19	Tillage operation	Generegic Conservation Tillage
1	6	9	Tillage operation	Generegic Conservation Tillage
1	6	30	Plant/begin. growing season	TEFF
1	7	1	Fertilizer application	Urea (100,0.2)
1	8	1	Fertilizer application	Urea (80,0.2)
1	11	30	Harvest and kill operation	
2	4	22	Tillage operation	Generegic Conservation Tillage
2	5	13	Plant/begin. growing season	GRSG
3	1	31	Harvest and kill operation	
3	8	11	Tillage operation	Generegic Conservation Tillage
3	9	1	Plant/begin. growing season	LECH (HU to maturity 2000)

Sorghum - Chickpea - Teff			141021GRSG applies for Subb: 16,26; & 10,23,30;	
Year	*Month*	*Day*	*Management operation*	*Specification*
1	4	22	Tillage operation	Generegic Conservation Tillage
1	5	13	Plant/begin. growing season	GRSG
2	1	31	Harvest and kill operation	
2	8	11	Tillage operation	Generegic Conservation Tillage
2	9	1	Plant/begin. growing season	LECH (HU to maturity 2000)
3	1	15	Harvest and kill operation	
3	4	28	Tillage operation	Generegic Conservation Tillage
3	5	19	Tillage operation	Generegic Conservation Tillage
3	6	9	Tillage operation	Generegic Conservation Tillage
3	6	30	Plant/begin. growing season	TEFF
3	7	1	Fertilizer application	Urea (100,0.2)
3	8	1	Fertilizer application	Urea (80,0.2)
3	11	30	Harvest and kill operation	

Chickpea - Teff - Sorghum			141021LECH	
Year	*Month*	*Day*	*Management operation*	*Specification*
1	1	31	Harvest and kill operation	
1	8	11	Tillage operation	Generegic Conservation Tillage
1	9	1	Plant/begin. growing season	LECH (HU to maturity 2000)
2	1	15	Harvest and kill operation	
2	4	28	Tillage operation	Generegic Conservation Tillage
2	5	19	Tillage operation	Generegic Conservation Tillage
2	6	9	Tillage operation	Generegic Conservation Tillage
2	6	30	Plant/begin. growing season	TEFF
2	7	1	Fertilizer application	Urea (100,0.2)
2	8	1	Fertilizer application	Urea (80,0.2)
2	11	30	Harvest and kill operation	
3	4	22	Tillage operation	Generegic Conservation Tillage
3	5	13	Plant/begin. growing season	GRSG

Sorghum - Faba Bean - Barley			140930GRSG_2 applies for Subb: 2,4,5,7,8,12,13,14,15,18,21,22,25;	
Year	*Month*	*Day*	*Management operation*	*Specification*
1	4	22	Tillage operation	Generegic Conservation Tillage
1	5	13	Plant/begin. growing season	GRSG
2	1	31	Harvest and kill operation	
2	5	11	Tillage operation	Generegic Conservation Tillage
2	6	1	Plant/begin. growing season	LEFA (HU to maturity 1200)
2	10	1	Harvest and kill operation	
3	3	30	Tillage operation	Generegic Conservation Tillage
3	4	20	Tillage operation	Generegic Conservation Tillage
3	5	11	Tillage operation	Generegic Conservation Tillage
3	6	1	Plant/begin. growing season	BARL
3	6	2	Fertilizer application	Urea (80,0.2)
3	10	1	Harvest and kill operation	

Wheat			140930SWHT	
Year	*Month*	*Day*	*Management operation*	*Specification*
1	3	30	Tillage operation	Generegic Conservation Tillage
1	4	20	Tillage operation	Generegic Conservation Tillage
1	5	11	Tillage operation	Generegic Conservation Tillage
1	6	1	Plant/begin. growing season	SWHT
1	6	2	Fertilizer application	Urea (100,0.2)
1	7	1	Fertilizer application	Urea (25,0.2)
1	10	15	Harvest and kill operation	

Barley - Sorghum - Faba Bean			140930BARL	
Year	*Month*	*Day*	*Management operation*	*Specification*
1	3	30	Tillage operation	Generegic Conservation Tillage
1	4	20	Tillage operation	Generegic Conservation Tillage
1	5	11	Tillage operation	Generegic Conservation Tillage
1	6	1	Plant/begin. growing season	BARL
1	6	2	Fertilizer application	Urea (80,0.2)
1	10	1	Harvest and kill operation	
2	4	22	Tillage operation	Generegic Conservation Tillage
2	5	13	Plant/begin. growing season	GRSG
3	1	31	Harvest and kill operation	
3	5	11	Tillage operation	Generegic Conservation Tillage
3	6	1	Plant/begin. growing season	LEFA (HU to maturity 1200)
3	10	1	Harvest and kill operation	

Faba Bean - Barley - Sorghum			140930LEFA	
Year	*Month*	*Day*	*Management operation*	*Specification*
1	1	31	Harvest and kill operation	
1	5	11	Tillage operation	Generegic Conservation Tillage
1	6	1	Plant/begin. growing season	LEFA (HU to maturity 1200)
1	10	1	Harvest and kill operation	
2	3	30	Tillage operation	Generegic Conservation Tillage
2	4	20	Tillage operation	Generegic Conservation Tillage
2	5	11	Tillage operation	Generegic Conservation Tillage
2	6	1	Plant/begin. growing season	BARL
2	6	2	Fertilizer application	Urea (80,0.2)
2	10	1	Harvest and kill operation	
3	4	22	Tillage operation	Generegic Conservation Tillage
3	5	13	Plant/begin. growing season	GRSG